

**Use of a Process Analysis Tool for Diagnostic Study on Fine Particulate Matter Predictions  
in the U.S. Part II: Process Analysis and Sensitivity Simulations**

Ping Liu<sup>a, b</sup> and Yang Zhang<sup>a, \*</sup>

<sup>a</sup> Department of Marine, Earth, and Atmospheric Sciences, North Carolina State University,  
Raleigh, NC 27695

<sup>b</sup> School of Environmental Science and Engineering, Shanghai Jiao Tong University, Shanghai,  
China

Shaocai Yu and Kenneth L. Schere  
Atmospheric Sciences Modeling Division, the U.S. Environmental Protection Agency,  
Research Triangle Park, NC

**Atmospheric Pollution Research**

**(in press, 2010, accepted on 8/17/2010).**

---

\* Corresponding author: Yang Zhang, Department of Marine, Earth, and Atmospheric Sciences, Campus Box 8208, North Carolina State University, Raleigh, NC 27695; phone number: (919) 515-9688; fax number: (919) 515-7802; e-mail: yang\_zhang@ncsu.edu

## ABSTRACT

Following the Part I paper that described an application of the U.S. EPA Models-3/Community Multiscale Air Quality (CMAQ) modeling system to the 1999 Southern Oxidants Study episode, this paper presents results from process analysis (PA) using the PA tool embedded in CMAQ and subsequent sensitivity simulations to estimate the impacts of major model uncertainties identified through PA. Aerosol processes and emissions are the most important production processes for  $PM_{2.5}$  and its secondary components, while horizontal and vertical transport and dry deposition contribute to their removal. Cloud processes can contribute the production of  $PM_{2.5}$  and  $SO_4^{2-}$  and the removal of  $NO_3^-$  and  $NH_4^+$ . The model biases in  $PM_{2.5}$  and its secondary inorganic components are found to correlate with aerosol processes and dry deposition at all sites from all networks and sometimes with emissions and cloud processes at some sites. Guided with PA results, specific uncertainties examined include the dry deposition of  $PM_{2.5}$  species and its precursors, the emissions of  $PM_{2.5}$  precursors, the cloud processes of  $SO_4^{2-}$ , and the gas-phase oxidation of  $SO_2$ . Adjusting the most influential processes/factors (i.e., emissions of  $NH_3$  and  $SO_2$ , dry deposition velocity of  $HNO_3$ , and gas-phase oxidation of  $SO_2$  by OH) is found to improve the model overall performance in terms of  $SO_4^{2-}$ ,  $NO_3^-$ , and  $NH_4^+$  predictions.

**Keywords: Fine Particulate Matter, MM5/CMAQ, Process Analysis, Sensitivity Study**

## 1. Introduction

Operational model evaluation for ozone ( $O_3$ ) and fine particles ( $PM_{2.5}$ ) simulated by regional air quality models such as the U.S. EPA Models-3/Community Multiscale Air Quality (CMAQ) modeling system (Binkowski and Roselle, 2003; Byun and Schere, 2006) using the observations from surface networks has been extensively performed. Fewer studies, however, focus on detailed diagnostic and process analysis (PA) that provide insights into the mechanism for their formation (e.g., Zhang et al., 2005b, 2009; Yu et al., 2008; Wang et al., 2009). Various probing tools have been developed to understand the roles of atmospheric physical and chemical processes in determining the fate of  $O_3$  and  $PM_{2.5}$  through more in-depth mechanistic analyses

and sensitivity studies (Zhang et al., 2005a). One such tool is the PA technique embedded in Lagrangian or Eulerian air quality models, which calculates the integrated rates for individual reactions and the mass changes of individual processes based on the species mass conservation equation (Jeffries and Tonnesen, 1994). It provides a useful probing tool to examine the formation mechanism of O<sub>3</sub> and PM<sub>2.5</sub> under different chemical regimes, and the governing processes for major pollutants (Zhang et al., 2005a). PA includes the Integrated Process Rates (IPRs) and Integrated Reaction Rates (IRRs). IPRs quantify the contributions of different physical and chemical processes to the ambient concentrations of the species of interest; IRRs quantify the chemical evolution of gaseous species. PA has been applied to study O<sub>3</sub> chemistry and transport (Jeffries and Tonnesen, 1994; Jang et al., 1995; Jiang et al., 2003; O'Neill and Lamb, 2005; Kwok et al., 2005; Tonse et al., 2008), the impacts of climate change on O<sub>3</sub> and particles (Hogrefe et al., 2005), particle number concentration and size distribution (Zhang et al., 2005b), and the dominant formation and removal process of PM<sub>2.5</sub> during different episode (Yu et al., 2008; Wang et al., 2009).

Following an evaluation of CMAQ for its application to the 1999 Southern Oxidants Study episode for the period of June 12-28 described in part I (Liu et al., 2009), a detailed PA is conducted using the PA tool in CMAQ. Guided by the PA results, several sensitivity simulations are designed to study the model responses to the uncertainties of major production and removal processes and reactions identified by IPRs and IRRs analyses for inorganic PM<sub>2.5</sub>, aiming to improve model performance. This part II paper presents results from PA and sensitivity studies and identifies several areas of improvement for an accurate simulation of regional O<sub>3</sub> and PM<sub>2.5</sub>.

## **2. Methodology**

In Eulerian grid models such as CMAQ, the mass continuity equation that is a system of partial differential equations (PDEs) is applied to calculate the time-rate changes of concentrations of chemical species (Seinfeld and Pandis, 2006):

$$\frac{\partial C_i}{\partial t} = \left( u \frac{\partial C_i}{\partial x} + v \frac{\partial C_i}{\partial y} + w \frac{\partial C_i}{\partial z} \right) - \left[ \frac{\partial}{\partial x} \left( K_x \frac{\partial C_i}{\partial x} \right) + \frac{\partial}{\partial y} \left( K_y \frac{\partial C_i}{\partial y} \right) + \frac{\partial}{\partial z} \left( K_z \frac{\partial C_i}{\partial z} \right) \right] + \left( \frac{\partial C_i}{\partial t} \right)_{emis} + \left( \frac{\partial C_i}{\partial t} \right)_{chem} + \left( \frac{\partial C_i}{\partial t} \right)_{drydep} + \left( \frac{\partial C_i}{\partial t} \right)_{cloud} \quad (1)$$

where  $\frac{\partial C_i}{\partial t}$  is the change of concentration of species  $i$  with time; the first term on the right-hand side of Eq. (1) is the advection in the  $x$ ,  $y$ , and  $z$  directions, and  $u$ ,  $v$ , and  $w$  are the wind velocity components in the three directions; the second term is the diffusion term and  $K_x$ ,  $K_y$ , and  $K_z$  are turbulent diffusivities; the remaining four terms are the rates of change of species concentration due to emissions, chemical reactions (the net effects of production and loss), dry deposition, and cloud processes, respectively. IPRs split Eq. (1) into several PDEs or ordinary differential equations (ODEs) to compute the rates of change of species concentration due to individual processes: horizontal transport, vertical transport, emissions, dry deposition, gas-phase chemistry, aerosol processes, cloud processes, and mass balance adjustment. Horizontal transport is the sum of horizontal advection and diffusion, and similarly, vertical transport is the sum of vertical advection and diffusion. Aerosol processes represent the net effect of aerosol thermodynamics, gas-to-particle mass transfer (e.g., homogeneous nucleation and condensation of sulfuric acid and organic carbon (OC) on preexisting particles), and coagulation within and between Aitken and accumulation modes. Cloud processes represent the net effect of cloud attenuation of photolytic rates, aqueous-phase chemistry, below- and in-cloud mixing, cloud scavenging, and wet deposition. The mass balance adjustment is used to compensate for the mass inconsistency of species. IRRs calculate the rates of change of species concentration due to 214 individual reactions for 72 species simulated in the Statewide Air Pollution Research Center Mechanism (SAPRC99, Carter, 2000), the gas-phase chemistry used in the CMAQ simulation. The IRRs of 214 reactions are grouped into 34 products according to the reactions for radical initiation, propagation, production, and termination, as listed in Table A-1 in the supplementary data. The IPRs and IRRs are calculated and analyzed for  $PM_{2.5}$  mass,  $PM_{2.5}$  composition, and gaseous precursors of secondary  $PM_{2.5}$ . The correlation of different processes and large model biases of

PM species is analyzed to identify the most influential processes to the model biases. The chemical regimes of O<sub>3</sub> chemistry (i.e., nitrogen oxides (NO<sub>x</sub> = NO + NO<sub>2</sub>) or volatile organic compounds (VOCs) – limited conditions) and chemistry of major gas-phase oxidants and PM<sub>2.5</sub> precursors are examined through IRRs analyses. Subsequent sensitivity simulations are conducted to characterize the model responses to the uncertainties of major production and removal processes and reactions identified by IPRs and IRRs analyses for inorganic PM<sub>2.5</sub>. Eight sites from the Southeastern Aerosol Research and Characterization (SEARCH) are selected to contrast surface and column IPRs analyses. These include four urban sites (i.e., Jefferson Street in Atlanta (JST), GA; North Birmingham (BHM), AL; Gulfport (GFP), MS; Pensacola (PNS), FL), three rural sites (i.e., Yorkville (YRK), GA; Centreville (CTR), AL; Oak Grove (OAK), MS), and one suburban site (i.e., Outlying field (OLF), FL).

### **3. Results and Discussions**

#### **3.1 IRRs Analyses**

Figure 1(a) shows the spatial distribution of the 15-day mean chemical production of total odd oxygen (O<sub>x</sub>) that is the sum of O<sub>3</sub>, ground state oxygen atom (O), excited oxygen atom (O<sup>1</sup>(D)), nitrogen dioxide (NO<sub>2</sub>), peroxyntic acid (HNO<sub>4</sub>), nitric acid (HNO<sub>3</sub>), nitrate radical (NO<sub>3</sub>), and dinitrogen pentoxide (N<sub>2</sub>O<sub>5</sub>) (i.e.,  $O_x = O_3 + O + O^1(D) + NO_2 + HNO_4 + HNO_3 + 2NO_3 + 3N_2O_5$ ). The total O<sub>x</sub> production is significant in the eastern U.S. and California, particularly along the Pacific coast, where high O<sub>3</sub> episodes usually occur. Two photochemical indicators are used to determine the VOC- or NO<sub>x</sub>-sensitive regimes: afternoon reactive nitrogen (NO<sub>y</sub>) recommended by Sillman (1995) and the ratio of production rates of peroxides (H<sub>2</sub>O<sub>2</sub>) and HNO<sub>3</sub> (P<sub>H<sub>2</sub>O<sub>2</sub></sub>/P<sub>HNO<sub>3</sub></sub>) proposed by Tonnesen and Dennis (2000). The former focuses on the NO<sub>x</sub>-VOC sensitivity of chemical concentration, and the afternoon NO<sub>y</sub> mixing ratio larger than 20 ppb indicates a VOC-sensitive chemistry (Sillman, 1995). The later focuses on the NO<sub>x</sub>-VOC sensitivity of instantaneous chemical production rate, and the value of P<sub>H<sub>2</sub>O<sub>2</sub></sub>/P<sub>HNO<sub>3</sub></sub> less than 0.06

at any time during the day indicates a VOC-sensitive chemistry (Tonnesen and Dennis, 2000). The photochemical indicators are useful to qualitatively identify NO<sub>x</sub>- and VOC-sensitive O<sub>3</sub> chemistry in the ambient atmosphere, though they are subject to some uncertainties, including uncertain dry/wet deposition rates, aerosol processes, measurement error, mechanism dependence, and case-to-case variations (Sillman and He, 2002). As shown in Figures 1(b) and 1(c), a few cities over the west coast of California, New England area, the Great Lakes, and Ohio valley in the mid-west are primarily dominated by VOC-sensitive chemistry, indicated by occurrences of NO<sub>y</sub> > 20 ppb and P<sub>H<sub>2</sub>O<sub>2</sub></sub>/P<sub>HNO<sub>3</sub></sub> < 0.06 over these regions. This is due to the relatively higher NO<sub>x</sub> emissions in those urban areas. By contrast, most rural and remote areas, where VOC emissions are high, are primarily dominated by NO<sub>x</sub>-sensitive chemistry. The ratio of P<sub>H<sub>2</sub>O<sub>2</sub></sub>/P<sub>HNO<sub>3</sub></sub> identifies slightly larger areas with VOC-sensitive chemistry than NO<sub>y</sub>, likely because the indicator involving H<sub>2</sub>O<sub>2</sub> appear to be more robust (Tonnesen and Dennis, 2000). The amount of hydroxyl radical (OH) consumed by VOCs to produce O<sub>3</sub> are analyzed in terms of their fractions reacting with anthropogenic and biogenic VOCs (AVOCs and BVOCs), as shown in Figure 2. OH radicals reacted with BVOCs are high in the southeastern U.S. and California; those reacted with AVOCs are high in the mid-west, Texas, and the west coast in California. The dominance of VOC emissions and their subsequent oxidations by OH radicals over most U.S. areas dictates the nature of the NO<sub>x</sub>-limited O<sub>3</sub> chemistry.

In SAPRC99, HNO<sub>3</sub>, a precursor of NO<sub>3</sub><sup>-</sup>, is formed or depleted via three major pathways:



where HC represents non-methane hydrocarbons such as aldehydes, glyoxal, and phenols. Two other pathways include the photolysis of HNO<sub>3</sub> and the reaction between NO<sub>3</sub> and HO<sub>2</sub>, which are relatively minor sink or source. Figure A-1 shows the daily totals of the production of HNO<sub>3</sub>

from reactions (2) and (3) and the depletion of  $\text{HNO}_3$  from reaction (4) at an urban (JST) and a rural site (YRK) in Georgia. As shown in Figure 7 in Part I, CMAQ simulates the temporal variation of  $\text{HNO}_3$  relatively well at JST. Significant overpredictions of  $\text{HNO}_3$  occur at YRK on June 22-23. On average, 98% and 95% of the production of  $\text{HNO}_3$  can be attributed to reaction (2) at JST and YRK, respectively. OH can consume  $\text{HNO}_3$  to produce  $\text{NO}_3$ , and the amount is less than 1% of total  $\text{HNO}_3$  production, indicating other dominant pathways such as dry and wet deposition may contribute mostly to the removal of  $\text{HNO}_3$  at both sites.

### **3.2 IPRs Analysis**

#### **3.2.1 Column and Export Analysis**

The IPRs are calculated as an average of hourly values for a column block of horizontal grid cells in the planetary boundary layer (PBL, defined to be layers 1-14, corresponding to 0-2.6 km above the ground level) at each site for the 15-day period, where the block is defined as the grid cell in which the site is located and its eight surrounding grid cells, because one grid cell cannot be viewed independently and the horizontal transport from the adjacent grid cells can play an important role in the variations of pollutant concentrations. The net domainwide average exports of air pollutants are calculated as the sum of process contributions of emissions, gas-phase chemistry, PM processes, cloud processes, and dry deposition in the PBL. The positive values indicate export out of the PBL into the free troposphere, and the negative values indicate import from the free troposphere into the PBL. The column IPRs represent the average exports in the PBL. 8 SEARCH sites are selected to analyze the IPRs, and they are grouped as urban sites (i.e., JST, BHM, GFP, and PNS) and rural or suburban sites (i.e., YRK, CTR, OAK, and OLF).

Figure 3 shows the process contributions of  $\text{PM}_{2.5}$ , sulfate ( $\text{SO}_4^{2-}$ ), nitrate ( $\text{NO}_3^-$ ), ammonium ( $\text{NH}_4^+$ ), and their precursors, sulfur dioxide ( $\text{SO}_2$ ),  $\text{HNO}_3$ , ammonia ( $\text{NH}_3$ ), and  $\text{NO}_x$  at SEARCH urban and rural sites. The process contributions of  $\text{PM}_{2.5}$  are similar to those of  $\text{SO}_4^{2-}$  except for emissions, because surface  $\text{SO}_4^{2-}$  accounts for most of  $\text{PM}_{2.5}$  mass with an average

range of 49% at both urban and rural sites, and the major sources of PM<sub>2.5</sub> emissions are elemental carbon (EC) and primary OC. The contributions of dry deposition to the removal of all species except for HNO<sub>3</sub> are relatively small. In both urban and rural areas, horizontal and vertical transports, dry deposition, and wet depositions remove the pollutants from the column and contribute to the loss of PM<sub>2.5</sub> and SO<sub>4</sub><sup>2-</sup>, while aerosol processes such as homogenous nucleation and condensation, cloud processes such as aqueous-phase chemistry, and emissions contribute to their production. The mass gain from aqueous-phase chemistry dominates over mass loss due to wet deposition, resulting in a net increase of their mass concentrations due to cloud processes. Unlike PM<sub>2.5</sub> and SO<sub>4</sub><sup>2-</sup>, horizontal transport contributes to the increase of NO<sub>3</sub><sup>-</sup> in the rural area, indicating an air mass with high NO<sub>3</sub><sup>-</sup> may have moved into the area. Aerosol processes contribute to the increase of NO<sub>3</sub><sup>-</sup> in both urban and rural areas, as a result of a complex gas-particle partitioning. Cloud processes contribute to the removal of NO<sub>3</sub><sup>-</sup> and NH<sub>4</sub><sup>+</sup> in both urban and rural areas, mainly due to the dominance of the in-cloud chemistry, cloud mixing and scavenging, and subsequent wet deposition. Vertical transport contributes to the removal NO<sub>3</sub><sup>-</sup> and NH<sub>4</sub><sup>+</sup> in both urban and rural areas, indicating that the air mass with high NO<sub>3</sub><sup>-</sup> and NH<sub>4</sub><sup>+</sup> may have been transferred into the column block. In general, aerosol and cloud processes are major contributors to the production of SO<sub>4</sub><sup>2-</sup>, and aerosol processes are a major contributor to the productions of NO<sub>3</sub><sup>-</sup> and NH<sub>4</sub><sup>+</sup>. Cloud processes dominate the removal of NO<sub>3</sub><sup>-</sup> and NH<sub>4</sub><sup>+</sup>. Dry deposition contributes to the removal of all species.

Emissions are important sources for PM precursors, including SO<sub>2</sub>, NO<sub>x</sub>, and NH<sub>3</sub>. Dry deposition is an important removal process for all PM precursors, particularly for HNO<sub>3</sub>. Gas-phase chemistry depletes SO<sub>2</sub> and NO<sub>x</sub> through their oxidation by OH radicals to form H<sub>2</sub>SO<sub>4</sub> and HNO<sub>3</sub>, respectively, but increases the level of precursors such as HNO<sub>3</sub>, via oxidation of NO<sub>2</sub> by OH during daytime and oxidation of HC by NO<sub>3</sub> during night, as shown in reactions (2) and (3). Aerosol processes contribute to a decrease in SO<sub>2</sub>, NO<sub>x</sub>, and NH<sub>3</sub> but an increase in

HNO<sub>3</sub>, indicating that the gas-particle equilibrium favors the volatility of NO<sub>3</sub><sup>-</sup> to the gas-phase to form HNO<sub>3</sub>. Cloud processes slightly contribute to the decrease of SO<sub>2</sub>, HNO<sub>3</sub>, NH<sub>3</sub>, and NO<sub>x</sub> through in-cloud chemistry, in- and below-cloud scavenging, and subsequent wet deposition. Most processes will be further examined in the correlation analysis in the next section.

The 15-day average of net domain-wide process contributions and exports of O<sub>x</sub>, O<sub>3</sub>, NO<sub>x</sub>, NO<sub>y</sub>, HNO<sub>3</sub>, SO<sub>2</sub>, AVOC, BVOC, and PM<sub>2.5</sub> from the PBL to free troposphere are summarized in Table 1. While the process contributions represent the net column (a total of 14 layers, corresponding to 0-2.6 km) concentration changes due to each process, the net export represents the total amount of pollutants that can be transported from PBL to the free troposphere. Relatively large amounts of O<sub>x</sub>, O<sub>3</sub>, AVOCs, and PM<sub>2.5</sub> can be exported from the PBL to the free troposphere. Such exports of pollutants enhance the total oxidation capacity in the middle and upper troposphere; they can thus affect the concentrations of pollutants at surface or in the PBL and modulate the local meteorology/climate in other regions. For example, the secondary pollutants in the upper troposphere can transport to the ground through vertical mixing, and aerosol feedbacks (e.g., direct effects via radiation reduction and indirect effects via serving as cloud condensation nuclei (CCN)) to PBL meteorology can affect temperature, relative humidity (RH), and wind field (Zhang, 2008) (though such feedbacks are not treated in the CMAQ used in this study).

### 3.2.2 IPRs Correlation Analysis

To further understand the relationship between model biases and major atmospheric processes that may provide guidance for sensitivity studies, the correlation of the large model errors and the contributions of individual processes are analyzed for PM<sub>2.5</sub>, SO<sub>4</sub><sup>2-</sup>, NO<sub>3</sub><sup>-</sup>, and NH<sub>4</sub><sup>+</sup> at the SEARCH, the Clean Air Status and Trends Network (CASTNET), the Interagency Monitoring of Protected Visual Environments (IMPROVE), and the Speciation Trends Network (STN) sites (where the large model error is defined as the absolute difference between predictions

and observations that is greater than 20%). It is assumed that if a particular process is highly correlated with the large errors, and this process may likely contribute to the model biases and will be examined further through sensitivity simulations.

Correlations of emission contributions of major PM<sub>2.5</sub> precursors (i.e., SO<sub>2</sub>, NO<sub>x</sub>, and NH<sub>3</sub>) versus PM biases are shown in Figure A-2. SO<sub>2</sub> and NH<sub>3</sub> emissions are correlated with SO<sub>4</sub><sup>2-</sup> and NH<sub>4</sub><sup>+</sup> biases at the SEARCH, IMPROVE, and CASTNET sites. NO<sub>x</sub> emissions are correlated with NO<sub>3</sub><sup>-</sup> biases at the IMPROVE and CASTNET sites, but slightly anti-correlated at the SEARCH sites, especially at the SEARCH urban sites. The correlations of process contributions from PM<sub>2.5</sub> precursors (i.e., SO<sub>2</sub>, HNO<sub>3</sub>, and NH<sub>3</sub>) versus major PM<sub>2.5</sub> components (i.e., SO<sub>4</sub><sup>2-</sup>, NO<sub>3</sub><sup>-</sup>, and NH<sub>4</sub><sup>+</sup>) biases are also analyzed. As shown in Figure 4, there are no obvious correlations found between cloud processes of all three precursors and aerosol processes of SO<sub>2</sub> and HNO<sub>3</sub> with PM biases. Dry deposition of SO<sub>2</sub> and HNO<sub>3</sub> are anti-correlated to the model biases for SO<sub>4</sub><sup>2-</sup> and NO<sub>3</sub><sup>-</sup>, respectively, at the IMPROVE and CASTNET sites. Dry deposition of NH<sub>3</sub> is anti-correlated with the NH<sub>4</sub><sup>+</sup> biases at the CASTNET sites (i.e., largely at rural sites), but slightly correlated at the SEARCH sites (i.e., urban and rural sites in the southeastern U.S.). Aerosol processes of NH<sub>3</sub> are anti-correlated with NH<sub>4</sub><sup>+</sup> biases at both the SEARCH and CASTNET sites, indicating the conversion of NH<sub>3</sub> to ammonium nitrate (NH<sub>4</sub>NO<sub>3</sub>). Moreover, aerosol processes may not be the major contributors to NH<sub>4</sub><sup>+</sup> overpredictions at the CASTNET and IMPROVE sites. NH<sub>3</sub> emissions are the largest contributors to the NH<sub>4</sub><sup>+</sup> biases (Figure A-2), especially at the CASTNET sites with a correlation coefficient (R) of 0.46.

Figure 5 shows the correlation between different processes (i.e., dry deposition, aerosol processes, and cloud processes) and large model biases for PM<sub>2.5</sub>, SO<sub>4</sub><sup>2-</sup>, NO<sub>3</sub><sup>-</sup>, and NH<sub>4</sub><sup>+</sup> at the SEARCH, IMPROVE and CASTNET sites. Similar plots at SEARCH sites accounting for all, urban or rural sites separately are also provided in Figure A-3. The R values between various processes and model biases for these species at all sites from SEARCH, IMPROVE, CASTNET,

and STN are given in Table 2. Horizontal transport is highly correlated with  $PM_{2.5}$  biases at the STN sites with an R value of 0.72 and slightly-to-moderately anti-correlated with biases of  $PM_{2.5}$  and its component at other sites. Vertical transport is correlated with  $SO_4^{2-}$  biases with R values of 0.42-0.45 at rural sites from SEARCH, IMPROVE, and CASTNET, and slightly-to-moderately correlated (most negatively) with biases in other species. Emissions are slightly-to-moderately correlated to  $PM_{2.5}$  and  $SO_4^{2-}$  biases at the SEARCH urban sites,  $PM_{2.5}$  and  $NO_3^-$  biases at the IMPROVE sites, and  $SO_4^{2-}$  and  $NO_3^-$  biases at the CASTNET sites. Dry deposition is anti-correlated with biases of  $PM_{2.5}$  and its inorganic components at all urban and rural sites (except for  $NO_3^-$  at the rural sites) with R values of -0.7 to -0.2. Higher dry deposition flux in terms of absolute values (ignoring the negative sign, which indicates a removal process) corresponds to higher simulated concentrations (i.e., the model overpredictions) because the deposition flux is proportional to the species concentration and deposition velocity. Aerosol processes are anti-correlated with  $NO_3^-$  biases at the SEARCH urban sites,  $NH_4^+$  biases at the SEARCH rural sites, and  $PM_{2.5}$  biases at the STN sites (with R values of -0.7 to -0.2), but positively correlated with biases in most species (with R values of 0.2 to 0.6) at the SEARCH and all species at the IMPROVE and CASTNET sites. Note that opposite correlations exist between aerosol processes and  $PM_{2.5}$  biases at STN vs. other networks and between aerosol processes and biases of  $NH_4^+$  and  $NO_3^-$  at the SEARCH urban vs. rural sites. To understand such opposite correlations, the IPRs correlation analyses are conducted under dry and wet conditions separately according to the amount of convective and non-convective rain (0 for dry or > 0 for wet). As shown in Figures A-4 to A-6 in the supplementary data, the large negative correlations (that correspond to large model biases) occur at a few sites mostly under dry conditions which dominate over those under wet conditions, causing a net negative correlation between aerosol processes and  $PM_{2.5}$  biases at the STN sites or  $NO_3^-$  biases at the SEARCH urban sites (e.g., a significant  $PM_{2.5}$  increase ( $2.5 \mu g m^{-3} day^{-1}$ ) from aerosol processes coincides with a significant

negative model bias ( $-22.3 \mu\text{g m}^{-3}$ ) on June 17 at north Long Beach site in the STN network). Negative correlations between aerosol processes and  $\text{NH}_4^+$  biases occur under both dry and wet conditions at the SEARCH rural sites where  $\text{NH}_3$  is rich. These results indicate large model biases likely occur in the PM model treatments (e.g., the inorganic thermodynamic equilibrium in ISORROPIA) under dry conditions or  $\text{NH}_3$ -rich conditions. Cloud processes are correlated with model biases for  $\text{PM}_{2.5}$  and  $\text{NH}_4^+$  at the SEARCH rural sites (with R values of 0.3 and 0.5, respectively) but anti-correlated with  $\text{SO}_4^{2-}$  at the IMPROVE sites and  $\text{NO}_3^-$  at the CASTNET sites, and  $\text{PM}_{2.5}$  at the STN sites (with R values of -0.3, -0.5, and -0.2, respectively).

### **3.3 Sensitivity Simulations**

The above PA results show that emissions, aerosol/cloud processes, and dry deposition of PM precursors may contribute to the model biases of the secondary PM. With the guidance from PA, several sensitivity simulations are subsequently conducted to analyze the model responses to  $\text{NO}_x$ - vs. VOC-limited regimes identified via IRRs and changes in key processes and reactions identified via IPRs, aiming to reduce model biases.

#### **3.3.1 $\text{NO}_x$ - vs. VOC- sensitivity of $\text{O}_3$ Chemistry**

Using the production rate of  $\text{H}_2\text{O}_2/\text{HNO}_3$  as a photochemical indicator,  $\text{O}_3$  formation over most U.S. is dominated by  $\text{NO}_x$ -sensitive chemistry, and California, New England, and the Great Lakes and Ohio valley in the mid-west are primarily dominated by VOC-sensitive chemistry (section 3.1). Two sensitivity simulations are conducted with 50% domain-wide reduction of  $\text{NO}_x$  and VOC emissions to simulate the responses of  $\text{O}_3$  mixing ratios to changes in its precursor emissions and verify whether the indicators are robust to distinguish  $\text{NO}_x$ - and VOC-sensitivity of  $\text{O}_3$  chemistry. Figure A-7 shows the spatial distributions of the absolute and percentage differences in 15-day mean of hourly  $\text{O}_3$  mixing ratios between sensitivity and baseline simulations. Reducing 50% VOC emissions results in lower  $\text{O}_3$  mixing ratios in California and the Great Lakes and Ohio valley in the mid-west, compared with baseline results. Reducing 50%

NO<sub>x</sub> emissions results in lower O<sub>3</sub> mixing ratios in most U.S., indicating a dominance of the NO<sub>x</sub>-sensitive O<sub>3</sub> chemistry over most U.S., consistent with results based on the photochemical indicators P<sub>H<sub>2</sub>O<sub>2</sub></sub>/P<sub>HNO<sub>3</sub></sub> described in section 3.1. However, increasing O<sub>3</sub> mixing ratios occur with 50% NO<sub>x</sub> emission reduction at some locations in California, mid-western, north eastern, and southern U.S., due either a VOC-limited O<sub>3</sub> chemistry or an accumulation of O<sub>3</sub> dominated by transport, or both over those areas. Such O<sub>3</sub> disbenefits from NO<sub>x</sub> emission control are also reported by Arnold and Dennis (2006) at JST using the SAPRC99 gas-phase mechanism and by Zhang et al. (2009) using the carbon bond (CB-IV) gas-phase mechanism.

### 3.3.2 Emissions of PM<sub>2.5</sub> Precursors

Emissions are a primary process that contributes to the increase of pollutant concentrations. The emissions used in this study are based on the U.S. EPA's 1999 National Emission Inventory (NEI) v. 3, processed by the Sparse Matrix Operator Kernel Emissions system (SMOKE) v. 1.4 by the U.S. EPA. The total emissions of NH<sub>3</sub>, an important precursor of NH<sub>4</sub><sup>+</sup>, is compared with the results from the Carnegie Mellon University (CMU) national NH<sub>3</sub> emission inventory (<http://www.cmu.edu/ammonia/>) (Goebes et al., 2003; Pinder et al., 2004) that is considered to be more accurate than the NEI v. 3 for several reasons (Wu et al., 2008). For example, the CMU NH<sub>3</sub> inventory provides the process-based, and temporally- and spatially-resolved estimates for fertilizer and dairy cattle. The dependence of NH<sub>3</sub> emissions on climate conditions, farming practice, and the geographic variation of animal population is taken into account in the CMU inventory. Compared with the CMU NH<sub>3</sub> inventory, NEI v. 3 used here gives NH<sub>3</sub> emissions that are lowered by 25.5% on average domain-wide for this episode. A factor of 1.2551 is therefore applied to adjust total NH<sub>3</sub> emission uniformly for the entire domain in the sensitivity simulation.

The results show that increased NH<sub>3</sub> emissions can cause increased NO<sub>3</sub><sup>-</sup> and NH<sub>4</sub><sup>+</sup> since more NH<sub>3</sub> is available to form NH<sub>4</sub>NO<sub>3</sub>. There are no significant impacts on SO<sub>4</sub><sup>2-</sup> and PM<sub>2.5</sub>. This is likely due to the sulfate-poor (i.e., NH<sub>3</sub>-rich; [NH<sub>4</sub><sup>+</sup>]/[SO<sub>4</sub><sup>2-</sup>] > 2) condition at those sites

(for example, both observed and simulated average  $[\text{NH}_4^+]/[\text{SO}_4^{2-}]$  is greater than 4 at the IMPROVE sites).  $\text{SO}_4^{2-}$  is neutralized by  $\text{NH}_3$ , and the increased  $\text{NH}_3$  is able to neutralize more  $\text{NO}_3^-$  (Ansari and Pandis, 1998; Takahama et al., 2004). Figures 6(a)-6(c) show the NMBs of simulated  $\text{PM}_{2.5}$ ,  $\text{SO}_4^{2-}$ ,  $\text{NO}_3^-$ , and  $\text{NH}_4^+$  against observations from the base simulation and the sensitivity simulation with adjusted  $\text{NH}_3$  and  $\text{SO}_2$  emissions. Increasing  $\text{NH}_3$  emissions can increase  $\text{NO}_3^-$  by 43-73%, and the NMBs of  $\text{NO}_3^-$  change from -45%, -75%, and -22% of the baseline simulation to -23%, -56%, and 14% of the sensitivity simulation at the IMPROVE, SEARCH, and CASTNET sites, respectively. The NMB of  $\text{NH}_4^+$  changes from -32% to -20% at the SEARCH sites, but from 24% to 42% at the IMPROVE sites and from 8% to 22% at the CASTNET sites (i.e., a worse performance) since  $\text{NH}_4^+$  is already overpredicted by the baseline simulation at these two sites. Those results indicate that increasing  $\text{NH}_3$  emission can significantly improve model performance of  $\text{NO}_3^-$  and  $\text{NH}_4^+$  when they are both underpredicted. Under such conditions,  $\text{NO}_3^-$  formation depends on the availability of  $\text{NH}_3$ .

Assuming that a linear relationship exists between the emissions of  $\text{SO}_2$  and  $\text{SO}_4^{2-}$  concentrations, a sensitivity simulation with 20% reduced  $\text{SO}_2$  emissions is conducted based on the baseline predictions of  $\text{SO}_4^{2-}$ . Although such a linear relationship is not always valid because the complex chemical reactions for the formation and depletion of  $\text{SO}_4^{2-}$  are nonlinear, the sensitivity simulation can help to understand how  $\text{SO}_2$  emissions affect PM simulations. Reducing  $\text{SO}_2$  emissions by 20% can reduce  $\text{SO}_4^{2-}$  by 15-16% and reduce the NMBs from 20% to 3%, 24% to 5%, and 18% to 1% at the IMPROVE, SEARCH, and CASTNET sites. Decreasing  $\text{SO}_4^{2-}$  makes more  $\text{NH}_3$  available to form  $\text{NH}_4\text{NO}_3$  (Ansari and Pandis, 1998; West et al., 1999; Blanchard et al., 2000), which increases the  $\text{NO}_3^-$  concentration but decreases the  $\text{NH}_4^+$  concentration due to the replacement of ammonium sulfate ( $(\text{NH}_4)_2\text{SO}_4$ ) to  $\text{NH}_4\text{NO}_3$ .

### **3.3.3 Dry Deposition**

#### **3.3.3.1 $\text{PM}_{2.5}$ Species**

Dry deposition is an important removal process for PM<sub>2.5</sub> species as shown in the IPRs analyses. Two methods are used to investigate the effects of dry deposition on major PM<sub>2.5</sub> species, especially SO<sub>4</sub><sup>2-</sup>: directly adjusting dry deposition velocity of SO<sub>4</sub><sup>2-</sup> and adjusting dry deposition flux of the accumulation mode with most fine SO<sub>4</sub><sup>2-</sup>. A 20% increase of SO<sub>4</sub><sup>2-</sup> dry deposition velocity or fluxes is applied in the above methods based on ~20% overprediction of SO<sub>4</sub><sup>2-</sup> in the baseline simulation. The impacts of these two adjustments are negligible for PM species simulations. For example, at the IMPROVE and CASTNET sites, simulated SO<sub>4</sub><sup>2-</sup> concentration only increases by 1% and the NMBs of SO<sub>4</sub><sup>2-</sup> are improved from 20% to 19% and from 18% to 17%. One possible reason is that the overprediction of SO<sub>4</sub><sup>2-</sup> concentration is so significant that makes the impact of increased dry deposition fluxes negligible, since the latter is proportional to the species concentration and deposition velocity. The impact of adjustment of deposition velocity is small relative to the concentration variations. Therefore, additional sensitivity simulation is conducted with both of reduced SO<sub>2</sub> emissions (as discussed in the previous section) and increased dry deposition velocity of SO<sub>4</sub><sup>2-</sup>. However, the statistic results show that the improvement of this simulation is equivalent to the sum of the improvement resulted from the two individual adjustments. Although the relations of deposition of PM species are identified in the IPR correlation analysis, there is no significant evidence showing in sensitivity simulations due to the nearly negligible magnitudes of the contributions from the deposition of PM species to model biases.

### 3.3.3.2 PM<sub>2.5</sub> Precursors

Dry deposition is a major removal process for PM<sub>2.5</sub> precursors (e.g., HNO<sub>3</sub>, SO<sub>2</sub>, and NH<sub>3</sub>). Three sensitivity simulations are set up to test the model responses to the dry deposition velocities of those precursors. The typical dry deposition velocities, V<sub>d</sub>, are 4 cm s<sup>-1</sup> over land for HNO<sub>3</sub> (Seinfeld and Pandis, 2006), 0.8~1.2 cm s<sup>-1</sup> in June for SO<sub>2</sub> (Finkelstein et al., 2000), and 3.94 ± 2.79 cm s<sup>-1</sup> during the day and 0.76 ± 1.69 cm s<sup>-1</sup> during nighttime in summer at North

Carolina (Phillips et al., 2004). Based on these observations, the simulated  $V_d$  values of  $\text{HNO}_3$ ,  $\text{SO}_2$ , and  $\text{NH}_3$  are adjusted by a factor of 0.5, 1.2, and 0.5, respectively, uniformly for the entire domain to examine the model sensitivity to changes in  $V_d$ .

As shown in Figures 6(d)-6(f), with a 50% reduction in the  $V_d$  of  $\text{HNO}_3$ , the NMBs of  $\text{NO}_3^-$  reduce from -45% to -29%, -75% to -69%, and -22% to -1% at the IMPROVE, SEARCH, and CASTNET sites, respectively, despite no significant change in the model performance for  $\text{NH}_4^+$ ,  $\text{SO}_4^{2-}$ , and  $\text{PM}_{2.5}$ . Compared with results from the baseline simulation, the sensitivity simulation with a reduced  $V_d$  of  $\text{HNO}_3$  gives higher  $\text{HNO}_3$  (by 38% on average), which in turn increases  $\text{NO}_3^-$  by 27%, 29%, and 22% at the IMPROVE, SEARCH, and CASTNET sites, respectively. The predictions for  $\text{NH}_4^+$ ,  $\text{SO}_4^{2-}$ , and  $\text{PM}_{2.5}$  generally remain the same as the baseline values, since  $\text{NO}_3^-$  constitutes a small fraction of total  $\text{PM}_{2.5}$  (i.e., about 3%) at the IMPROVE and SEARCH sites. Reduction of the  $V_d$  of  $\text{NH}_3$  by 50% can increase  $\text{NO}_3^-$  by 18-21% and reduce the NMBs of  $\text{NO}_3^-$  from 45% to 35%, 75% to 70%, and 22% to 8% at the IMPROVE, SEARCH, and CASTNET sites, respectively. However, the NMB of  $\text{NH}_4^+$  increases from 24% to 31% at the IMPROVE sites, and similar effects can be found at the SEARCH and CASTNET sites but with small magnitudes. Under conditions with sufficient  $\text{NO}_x$  and low sulfate (e.g., sulfate-poor conditions), increased  $\text{NH}_3$  mixing ratios can cause increased  $\text{NH}_4^+$  and  $\text{NO}_3^-$ , since more  $\text{NH}_4\text{NO}_3$  can be formed following the formation of  $(\text{NH}_4)_2\text{SO}_4$ .  $\text{SO}_4^{2-}$  decreases about 2% and reduces the NMBs from 20% to 17%, 24% to 21%, and 18% to 15% at the IMPROVE, SEARCH, and CASTNET sites when  $V_d$  of  $\text{SO}_2$  is increased by 20%. It gives a slightly better model performance for  $\text{NO}_3^-$  at the IMPROVE, SEARCH, and CASTNET sites, as a result of higher predicted  $\text{NO}_3^-$  concentrations by 2-4%. The reduction of  $\text{SO}_4^{2-}$  can increase  $\text{NO}_3^-$  because it frees up  $\text{NH}_3$  to neutralize  $\text{HNO}_3$ ; however it cannot improve the underpredictions of  $\text{NH}_4^+$  as it causes a decrease in  $\text{NH}_4^+$  concentrations at the SEARCH sites.

### 3.3.4 Cloud Processes of $\text{SO}_4^{2-}$ and Gas-Phase Chemistry of $\text{SO}_2$

Cloud processes (e.g., dissolution of soluble gases, aqueous chemistry, scavenging, and wet deposition) have important impacts on  $\text{SO}_4^{2-}$  formation via the  $\text{SO}_2$  oxidations in the cloud droplet. Such an oxidation depends on the cloud liquid water content, pH, the concentrations of dissolved  $\text{O}_3$  and  $\text{H}_2\text{O}_2$ , and cloud lifetime (Seinfeld and Pandis, 2006; Mueller et al., 2006). In this study, simulated cloud fractions are compared with the observations from the Automated Surface Observing System (ASOS) at 13 sites available in the southeastern U.S. ASOS contains the surface observations of hourly data for cloud height and coverage that can be converted to cloud fraction. The comparison shows that MM5 overestimates observed cloud fractions by roughly 10% (simulated value of 0.403 vs. observed value of 0.376). Since adjusting cloud fractions in the meteorological inputs may cause a self-inconsistency in the meteorological fields, we adjust the dissolved concentrations of  $\text{H}_2\text{O}_2$  in cloud droplets using a dissolution efficiency factor that reflects the changes of cloud fractions. This adjustment will likely affect  $\text{SO}_4^{2-}$  formation since dissolved  $\text{SO}_2$  may be oxidized by aqueous oxidants such as  $\text{H}_2\text{O}_2$  in cloud droplets (Jayne et al., 1990). A dissolution efficiency factor of 0.9 is used for the sensitivity simulation. As shown in Figures 6(g)-6(i), the NMBs of  $\text{SO}_4^{2-}$  are slightly improved at the IMPROVE, SEARCH, and CASTNET sites (from 20% to 18%, 24% to 22%, and 18% to 16%, respectively). However, the mean  $\text{SO}_4^{2-}$  concentrations predicted in this sensitivity simulation only decrease by 1% at all three sites compared with those from the baseline simulation. This indicates that a 10% reduction of dissolved  $\text{H}_2\text{O}_2$  has negligible effects on  $\text{SO}_4^{2-}$  for this episode, due partly to the relatively scattered cloud conditions.

Another important formation of  $\text{SO}_4^{2-}$  is the gas-phase oxidation of  $\text{SO}_2$  by OH. The rate constant of this reaction used in SAPRC99 is larger than that used in CB05 (Yarwood et al., 2005; Luecken et al., 2005; Sarwar et al., 2008), especially under conditions with relatively low temperatures and high pressures, since this oxidation reaction depends both of them. For example, when temperature is 288 K and pressure is 1013 Pa, the rate constant of SAPRC99 is

1.12 times of that of CB05. One sensitivity simulation is conducted by replacing the rate constant by that used in CB05. Using the rate constant in CB05 for the  $\text{SO}_2(\text{g}) + \text{OH}$  reaction can reduce  $\text{SO}_4^{2-}$  by 3% and reduce NMB from 20% to 17%, 24% to 20%, and 18% to 13%, respectively, at the IMPROVE, SEARCH, and CASTNET networks.

Among the above sensitivity simulations, adjusting  $\text{NH}_3$  emissions and dry deposition velocity of  $\text{HNO}_3$  lead to the most improvement to  $\text{NO}_3^-$  statistics, while adjusting  $\text{SO}_2$  emissions and using the rate constant in CB05 for the  $\text{SO}_2(\text{g}) + \text{OH}$  reaction improve the  $\text{SO}_4^{2-}$  statistics the most. Finally, multiple adjustments are applied to one simulation to study the combined effects of those adjustments. The multiple adjustments are selected based on the individual sensitivity test that has the NMB improvement larger than 5%, including  $1.2551 \times E_{\text{NH}_3}$ ,  $0.8 \times E_{\text{SO}_2}$ ,  $K_{\text{SO}_2+\text{OH}}$ ,  $\text{CB05}$ , and  $0.84 \times V_{\text{d, HNO}_3}$ . As shown in Figures 6(j)-6(l), in this final simulation,  $\text{SO}_4^{2-}$  concentration is reduced by 16-19% and its NMBs are reduced from 20% to 1%, 24% to 3%, and 18% to 4%, respectively, at the IMPROVE, SEARCH, and CASTNET networks.  $\text{NO}_3^-$  concentration is increased by 74-127%. Its NMBs change from -45%, -75%, -22% to -12%, -42%, 33% at the IMPROVE, SEARCH, and CASTNET sites, respectively.  $\text{NH}_4^+$  concentration is increased by 1-8%, and its NMB is reduced from 32% to 27% at the SEARCH sites, but increased from 24% to 29% and from 8% to 9% at the IMPROVE and CASTNET sites. These statistics indicate an overall improvement of the model performance for  $\text{SO}_4^{2-}$  and  $\text{NO}_3^-$ , although the performance for  $\text{PM}_{2.5}$  is slightly worse. Reducing model biases in individual PM compositions is meaningful, because a “seemly” good performance in  $\text{PM}_{2.5}$  (e.g., in the baseline, compared with the sensitivity simulations with multiple adjustments) may result from a cancellation of positive and negative biases.

#### 4. Summary

Process analysis is performed to understand governing chemical and physical atmospheric processes for key pollutants in order to reduce model biases. The  $\text{O}_3$  chemistry regimes are

examined by using the ratio of production rates of  $\text{H}_2\text{O}_2$  and  $\text{HNO}_3$  from the IRR products during day time and  $\text{NO}_y$  concentrations during afternoon as photochemical indicators. The results show a dominance of  $\text{NO}_x$ -sensitive chemistry over most U.S., and a dominance of VOC-sensitive chemistry in major cities in the California, New England, and the Great Lakes and Ohio valley in the mid-west. The IPRs show the relatively large net amount of exported  $\text{O}_x$ ,  $\text{O}_3$ , AVOCs, and  $\text{PM}_{2.5}$  from the PBL to the free troposphere, which can further affect the chemical concentrations at the surface at downwind locations. Emissions are important sources for PM precursors such as  $\text{SO}_2$ ,  $\text{NO}_x$ , and  $\text{NH}_3$ . While cloud processes contribute to the decrease of  $\text{SO}_2$ ,  $\text{HNO}_3$ ,  $\text{NH}_3$ , aerosol processes contribute to a decrease in  $\text{SO}_2$ ,  $\text{NO}_x$ , and  $\text{NH}_3$  but an increase in  $\text{HNO}_3$ . Horizontal transport and dry deposition are important removal processes for all PM precursors, particularly for  $\text{HNO}_3$ . Aerosol processes and emissions are the most important production processes for  $\text{PM}_{2.5}$  and its secondary components, while horizontal and vertical transport and dry deposition contribute to their removal. Cloud processes can contribute to the production of  $\text{PM}_{2.5}$  and  $\text{SO}_4^{2-}$  and the removal of  $\text{NO}_3^-$  and  $\text{NH}_4^+$ .

The IPRs correlation analysis is conducted for  $\text{PM}_{2.5}$ ,  $\text{SO}_4^{2-}$ ,  $\text{NO}_3^-$ ,  $\text{NH}_4^+$ , and their precursors,  $\text{HNO}_3$ ,  $\text{NH}_3$ , and  $\text{SO}_2$  at the SEARCH, IMPROVE, and CASTNET sites. Horizontal transport is highly correlated with  $\text{PM}_{2.5}$  biases at the STN sites. Vertical transport is correlated with  $\text{SO}_4^{2-}$  at rural sites from SEARCH, IMPROVE, and CASTNET. Emissions are slightly-to-moderately correlated to  $\text{PM}_{2.5}$ ,  $\text{SO}_4^{2-}$ , and  $\text{NO}_3^-$  biases at some sites. Aerosol processes are correlated with the biases of  $\text{PM}_{2.5}$ ,  $\text{SO}_4^{2-}$ ,  $\text{NO}_3^-$ , and  $\text{NH}_4^+$  at all sites from all networks, with larger model biases occurring for  $\text{PM}_{2.5}$ ,  $\text{NO}_3^-$ , and  $\text{NH}_4^+$  under dry or  $\text{NH}_3$ -rich conditions. Cloud processes are sometimes correlated with a few species such as  $\text{PM}_{2.5}$  and  $\text{NH}_4^+$  at SEARCH rural sites,  $\text{SO}_4^{2-}$  at the IMPROVE sites, and  $\text{NO}_3^-$  at the CASTNET sites. Dry deposition is correlated with biases for all species, in particular  $\text{SO}_4^{2-}$  at all sites and  $\text{NO}_3^-$  at the IMPROVE and CASTNET sites. Guided from the PA results, several sensitivity simulations

are performed to quantify the model response to major processes/reactions contributing to the model biases. The variables/processes examined in these sensitivity simulations include the dry deposition velocities of PM species (i.e.,  $\text{SO}_4^{2-}$ ) and precursors (i.e.,  $\text{HNO}_3$ ,  $\text{NH}_3$ , and  $\text{SO}_2$ ), the emissions of PM precursors (i.e.,  $\text{NH}_3$  and  $\text{SO}_2$ ), and the cloud processes and gas-phase chemistry of  $\text{SO}_4^{2-}$  formation (e.g., the aqueous-phase oxidation of  $\text{SO}_2$  in the presence of  $\text{H}_2\text{O}_2$  and cloud and gas-phase oxidation of  $\text{SO}_2$  by  $\text{OH}$ ). The decreased dry deposition velocities of  $\text{HNO}_3$  and  $\text{NH}_3$  can increase  $\text{NO}_3^-$  and  $\text{NH}_4^+$  formation, therefore appreciably improving  $\text{NO}_3^-$  and  $\text{NH}_4^+$  predictions when they both are underpredicted. Higher dry deposition velocity of  $\text{SO}_2$  can increase  $\text{NO}_3^-$  and reduce  $\text{NH}_4^+$ , which can slightly improve model performance at the IMPROVE sites, but cannot improve the underpredictions of  $\text{NH}_4^+$  at the SEARCH sites. Adjusting  $\text{SO}_4^{2-}$  dry deposition alone or together with  $\text{SO}_2$  emissions reduction has negligible impacts on  $\text{PM}_{2.5}$  simulations especially for  $\text{SO}_4^{2-}$ . For this summer episode, when  $\text{NH}_3$  emission is increased, both  $\text{NO}_3^-$  and  $\text{NH}_4^+$  increase while  $\text{SO}_4^{2-}$  remains relatively constant, indicating the sulfate-poor conditions at both the IMPROVE and SEARCH sites. Similarly to the cases with decreased dry deposition velocities of  $\text{HNO}_3$  and  $\text{NH}_3$ , increased  $\text{NH}_3$  emissions can appreciably improve the model performance when both  $\text{NO}_3^-$  and  $\text{NH}_4^+$  are underpredicted. Reducing  $\text{SO}_2$  emissions can reduce  $\text{SO}_4^{2-}$  by 15-16%, and reduce the absolute NMB by 79-94%. The sensitivity simulation with a dissolution efficiency factor of  $\text{H}_2\text{O}_2$  shows that a 10% reduction of dissolved  $\text{H}_2\text{O}_2$  cannot significantly affect the  $\text{SO}_4^{2-}$  formation for this episode. Using the rate constant from CB05 for  $\text{SO}_2(\text{g}) + \text{OH}$  can reduce  $\text{SO}_4^{2-}$  by 3% and reduce the absolute NMB by 15-85%. Adjusting the most influential processes/factors (i.e., emissions of  $\text{NH}_3$  and  $\text{SO}_2$ , dry deposition velocity of  $\text{HNO}_3$ , and gas-phase oxidation of  $\text{SO}_2$  by  $\text{OH}$ ) improves the model overall performance in terms of  $\text{SO}_4^{2-}$ ,  $\text{NO}_3^-$ , and  $\text{NH}_4^+$  (e.g., reducing NMBs from 24% to 3%, -75% to -42%, and 32% to 27% at the SEARCH sites, respectively). These results suggest that improving treatments of these most influential processes/factors may help improve model performance.

## **Acknowledgements and Disclaimer**

This work was performed under the National Science Foundation Award No. Atm-0348819, and the Memorandum of Understanding between the U.S. Environmental Protection Agency (EPA) and the U.S. Department of Commerce's National Oceanic and Atmospheric Administration (NOAA) and under agreement number DW13921548. The authors thank Alice Gilliland and Steve Howard, U.S. NOAA/EPA, for providing the Fortran code for extracting data from CMAQ and the CASTNET, IMPROVE, and AIRS-AQS observational datasets, and Robert W. Pinder and Prakash Bhave, U.S. NOAA/EPA, for helpful discussions. Although this work was reviewed by EPA and approved for publication, it does not necessarily reflect their policies or views.

## References

- Ansari, A. S., and S. N. Pandis (1998), Response of inorganic PM<sub>2.5</sub> to precursor concentrations, *Environ. Sci. and Technol.*, *32*, 2706-2714.
- Arnold, J. R., and R. L. Dennis (2006), Testing CMAQ chemistry sensitivities in base case and emissions control runs at SEARCH and SOS99 surface sites in the southeastern US, *Atmos. Environ.*, *40*(26), 5027-5040.
- Binkowski, F. S., and S. J. Roselle (2003), Models-3 Community Multiscale Air Quality (CMAQ) Model aerosol component, 1. Model description, *J. Geophys. Res.*, *108*, 4183, doi:10.1029/2001JD001409.
- Blanchard, C. L., P. M. Roth, S. J. Tanenbaum, S. D. Ziman, and J. H. Seinfeld (2000), The use of ambient measurements to identify which precursor species limit aerosol nitrate formation, *J. Air & Waste Manage. Assoc.*, *50*, 2073-2084.
- Byun, D. W., and K. L. Schere (2006), Review of the governing equations, computational algorithms, and other components of the Models-3 Community Multiscale Air Quality (CMAQ) Modeling System, *Appl. Mech. Rev.*, *59*(2), 51-77.
- Carter, W. P. L. (2000), Implementation of the SAPRC99 chemical mechanism into the Models-3 Framework, Report to the US Environmental Agency, <ftp://ftp.cert.ucr.edu/pub/carter/pubs/s99mod3.pdf>.
- Finkelstein, P. L., T. G. Ellestad, J. F. Clarke, T. P. Meyers, D. B. Schwede, E. O. Hebert, and J. A. Neal (2000), Ozone and sulfur dioxide dry deposition to forests: Observations and model evaluation, *J. Geophys. Res.*, *105*(D12), 15365-15377.
- Goebes, M. D., R. Strader, and C. Davidson (2003), An ammonia emission inventory for fertilizer application in the United States, *Atmos. Environ.*, *37*(18), 2539-2550.
- Hogrefe, C., B. Lynn, C. Rosenzweig, R. Goldberg, K. Civerolo, J.-Y. Ku, J. Rosenthal, K. Knowlton, and P. L. Kinney (2005), Utilizing CMAQ process analysis to understand the impacts of climate change on ozone and particulate matter, the 4<sup>th</sup> Annual CMAS Models-3 User's Conference, Sept 26-28, Chapel Hill, NC.
- Jang, J.-C. C., H. E. Jeffries, and S. Tonnesen (1995), Sensitivity of ozone to model grid resolution-II. Detailed process analysis for ozone chemistry, *Atmos. Environ.*, *29*, 3101-3114.
- Jayne, J. T., J. A. Gardner, P. Davidovits, D. R. Worsnop, M. S. Zahniser, and C. E. Kolb (1990), The effect of H<sub>2</sub>O<sub>2</sub> content on the uptake of SO<sub>2</sub>(g) by aqueous droplets, *J. Geophys. Res.*, *95*(D12), 20559-20563.

- Jeffries, H. E., and S. Tonnesen (1994), A comparison of two photochemical reaction mechanisms using a mass balance and process analysis, *Atmos. Environ.*, 28, 2991-3003.
- Jiang, G., B. Lamb, and H. Westberg (2003), Using back trajectories and process analysis to investigate photochemical ozone production in the Puget Sound region, *Atmos. Environ.*, 37, 1489-1502.
- Kwok, R., J. C. H. Fung, J.-P. Huang, A. K. H. Lau, J. Lo, Z. Wang, and Y. Qin (2005), Comparison of CMAQ and SAQM using process analysis for Hong Kong ozone episodes, the 4th Annual CMAS Models-3 User's Conference, Sept 26-28, Chapel Hill, NC.
- Luecken, D., G. Yarwood, S. Rao, M. Yocke, G. Z. Whitten, and S. Reyes (2005), Updates to the carbon bond chemical mechanism: CB05, RT-04-00675, Novato, CA.
- Mueller, S. F., E. M. Bailey, T. M. Cook, and Q. Mao (2006), Treatment of clouds and the associated response of atmospheric sulfur in the Community Multiscale Air Quality (CMAQ) modeling system, *Atmos. Environ.*, 40(35), 6804-6820.
- O'Neill, S. M., and B. K. Lamb (2005), Intercomparison of the Community Multiscale Air Quality Model and CALGRID using process analysis, *Environ. Sci. Technol.*, 39, 5742-5753.
- Phillips, S. B., S. P. Arya, and V. P. Aneja (2004), Ammonia flux and dry deposition velocity from near-surface concentration gradient measurements over a grass surface in North Carolina, *Atmos. Environ.*, 38, 3469-3480.
- Pinder, R. W., R. Strader, C. I. Davidson, P. J. Adams (2004), A temporally and spatially resolved ammonia emission inventory for dairy cows in the United States, *Atmos. Environ.*, 38 (23), 3747-3756.
- Sarwar, G., D. Luecken, G. Yarwood, G. Whitten, and W. P. L. Carter (2008), Impact of an updated Carbon Bond Mechanism on predictions from the Community Multiscale Air Quality Model, *J. Appl. Met. Climatol.*, 47, 3-14.
- Seinfeld, J.H., and S.N. Pandis (2006), Atmospheric chemistry and physics: from air pollution to climate change, John Wiley and Sons, New York, NY.
- Sillman, S. (1995), The use of  $\text{NO}_y$ ,  $\text{H}_2\text{O}_2$  and  $\text{HNO}_3$  as indicators for  $\text{O}_3$ - $\text{NO}_x$ -VOC sensitivity in urban locations, *J. Geophys. Res.*, 100, 14175-14188.
- Sillman, S., and D. He (2002), Some theoretical results concerning  $\text{O}_3$ - $\text{NO}_x$ -VOC chemistry and  $\text{NO}_x$ -VOC indicators, *J. Geophys. Res.*, 107(D22), 4659, doi:10.1029/2001JD001123.
- Takahama, S., A. E., Witting, D. V. Vayenas, C. I. Davidson, and S. N. Pandis (2004), Modeling the diurnal variation of nitrate during the Pittsburgh air quality study. *J. Geophys. Res.*, 109, D16S06.

- Tonnesen, G. S., and R. L. Dennis (2000), Analysis of radical propagation efficiency to assess ozone sensitivity to hydrocarbons and NO<sub>x</sub>. Part 1: Local indicators of odd oxygen production sensitivity, *J. Geophys. Res.*, *105*, 9213-9225.
- Tonse, S. R., N. J. Brown, R. A. Harley, and L. Jin (2008), A process-analysis based study of the ozone weekend effect, *Atmos. Environ.*, *42*(33), 7728-7736.
- Wang, K., Y. Zhang, C. J. Jang, S. Phillips, and B.-Y. Wang (2009), Modeling study of intercontinental air pollution transport over the trans-Pacific region in 2001 using the Community Multiscale Air Quality (CMAQ) modeling system, *J. Geophys. Res.*, in press.
- West, J. J., A. S. Ansari, and S. N. Pandis (1999), Marginal PM<sub>2.5</sub>: nonlinear aerosol mass response to sulfate reductions in the eastern United States, *J. Air & Waste Manage. Assoc.*, *49*, 1415-1424.
- Wu, S.-Y., J.-L., Hu, Y. Zhang, and V. P. Aneja (2008), Modeling atmospheric transport and fate of ammonia in North Carolina, Part II. effect of ammonia emissions on fine particulate matter formation, *Atmos. Environ.*, *42*, 3437-3451.
- Yarwood, G., S. Rao, M. Yocke, and G. Whitten (2005), *Updates to the Carbon Bond Chemical Mechanism: CB05*, Final Report to the U.S. EPA, RT-04-00675, RTP, NC. [http://www.camx.com/publ/pdfs/CB05\\_Final\\_Report\\_120805.pdf](http://www.camx.com/publ/pdfs/CB05_Final_Report_120805.pdf).
- Yu, S., R. Mathur, K. Schere, D. Kang, J. Pleim, J. Young, D. Tong, G. Pouliot, S. A. McKeen, and S. T. Rao (2008), Evaluation of real-time PM<sub>2.5</sub> forecasts and process analysis for PM<sub>2.5</sub> formation over the eastern United States using the Eta-CMAQ forecast model during the 2004 ICARTT study, *J. Geophys. Res.*, *113*, D06204, doi:10.1029/2007JD009226.
- Zhang, Y. (2008), Online coupled meteorology and chemistry models: history, current status, and outlook, *Atmos. Chem. Phys.*, *8*, 2895-2932.
- Zhang, Y., K. Vijayaraghavan, and C. Seigneur (2005a), Evaluation of three probing techniques in a three-dimensional air quality model, *J. Geophys. Res.*, *110*, D02305, doi:10.1029/2004JD005248.
- Zhang, Y., P. Liu, K. Wang, M. Z. Jacobson, P. V. Bhave, S. Yu, S. J. Roselle, and K. L. Schere (2005b), Predicting aerosol number and size distribution with CMAQ: Homogeneous nucleation algorithms and process analysis, the 4<sup>th</sup> Annual CMAS Models-3 User's Conference, Sept 26-28, Chapel Hill, NC.
- Zhang, Y., X.-Y. Wen, K. Wang, K. Vijayaraghavan, and M. Z. Jacobson (2009), Probing into regional O<sub>3</sub> and PM pollution in the U.S., Part II. An examination of formation mechanisms through a process analysis technique and sensitivity study, *J. Geophys. Res.*, in press.

Table 1. The net domain-wide export of O<sub>x</sub>, O<sub>3</sub>, NO<sub>x</sub>, NO<sub>y</sub>, HNO<sub>3</sub>, SO<sub>2</sub>, AVOC, BVOC, and PM<sub>2.5</sub> from the planetary boundary layer (PBL) to the free troposphere during June 14-28, 1999, the unit is G mole/day for gas species and G gram/day for PM species.

Process	O <sub>x</sub>	O <sub>3</sub>	NO <sub>x</sub>	NO <sub>y</sub>	HNO <sub>3</sub>	SO <sub>2</sub>	AVOC	BVOC	PM <sub>2.5</sub>
Dry deposition	-5.21	-4.70	-0.11	-0.54	-0.35	-0.15	-0.97	0.00	-2.02
Gas-phase chemistry	6.39	5.18	-1.16	-0.17	0.50	-0.13	-2.20	-9.69	0.00
Aerosol processes	-0.06	0.00	0.00	0.00	0.12	0.00	0.00	0.00	20.50
Aqueous processes	0.25	0.55	-0.09	-0.30	-0.15	-0.36	-1.12	-0.34	-10.30
Emissions	0.06	0.00	1.43	1.43	0.00	0.72	6.86	10.65	12.01
Net export	1.44	1.03	0.07	0.42	0.12	0.08	2.57	0.61	20.19

Table 2. Correlation coefficient (R) of different processes and model biases in various species concentrations simulated by CMAQ.

Processes	SEARCH								IMPROVE				CASTNET			STN
	Urban Sites				Rural Sites				PM <sub>2.5</sub>	SO <sub>4</sub> <sup>2-</sup>	NO <sub>3</sub> <sup>-</sup>	NH <sub>4</sub> <sup>+</sup>	SO <sub>4</sub> <sup>2-</sup>	NO <sub>3</sub> <sup>-</sup>	NH <sub>4</sub> <sup>+</sup>	PM <sub>2.5</sub>
	PM <sub>2.5</sub>	SO <sub>4</sub> <sup>2-</sup>	NO <sub>3</sub> <sup>-</sup>	NH <sub>4</sub> <sup>+</sup>	PM <sub>2.5</sub>	SO <sub>4</sub> <sup>2-</sup>	NO <sub>3</sub> <sup>-</sup>	NH <sub>4</sub> <sup>+</sup>								
Horizontal Transport	-0.42	-0.30	-0.19	-0.29	0.05	-0.24	-0.20	-0.08	-0.20	-0.06	-0.34	-0.24	-0.19	-0.06	-0.30	0.72
Vertical Transport	-0.36	0.28	0.29	-0.29	-0.01	0.45	-0.10	0.10	-0.12	0.47	-0.41	-0.22	0.42	-0.17	-0.39	-0.04
Emissions	0.40	0.25	-0.08	--	0.01	-0.10	0.06	--	0.15	0.11	0.27	--	0.25	0.18	--	-0.07
Dry Deposition	-0.53	-0.58	-0.34	-0.40	-0.64	-0.71	0.05	-0.21	-0.20	-0.66	-0.72	-0.31	-0.61	-0.62	-0.42	-0.23
Aerosol Processes	0.35	0.12	-0.17	0.30	0.20	0.47	0.10	-0.18	0.17	0.35	0.40	0.40	0.60	0.25	0.42	-0.72
Clouds Processes	-0.04	-0.03	-0.04	-0.05	0.30	0.12	-0.01	0.47	-0.04	-0.27	-0.06	0.16	-0.04	-0.51	-0.04	-0.24

Note: "--" indicates no direct process contributions for emissions, since NH<sub>4</sub><sup>+</sup> is a secondary pollutant.

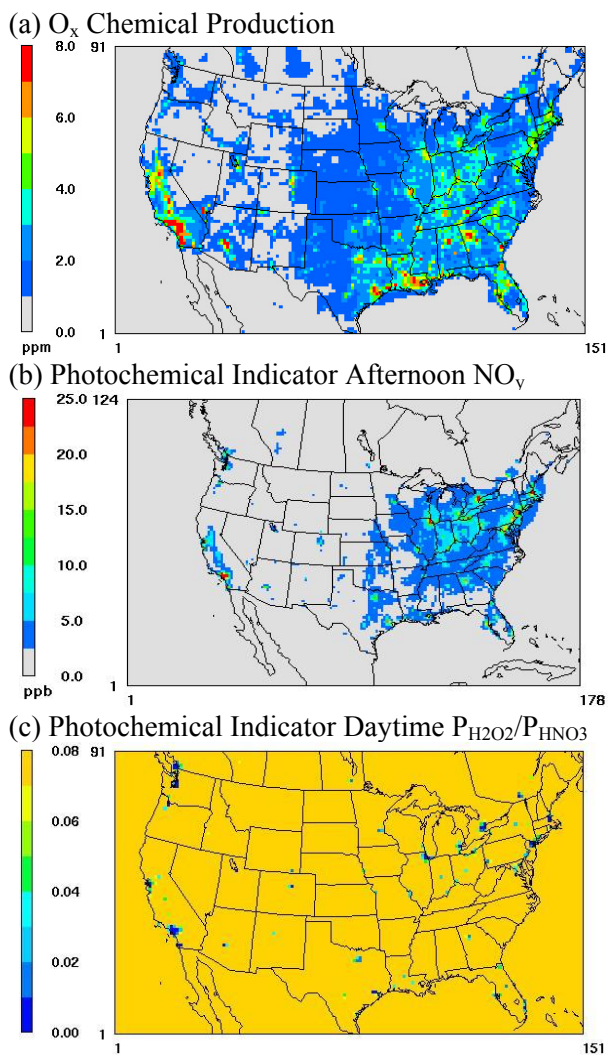


Figure 1. Spatial distributions of 15-day mean of (a) total  $O_x$  chemical production and photochemical indicator of (b)  $NO_v$  (ppb) during afternoon (1:00-5:00 pm) and (c)  $P_{H_2O_2}/P_{HNO_3}$  during daytime predicted by CMAQ during June 14-28, 1999.

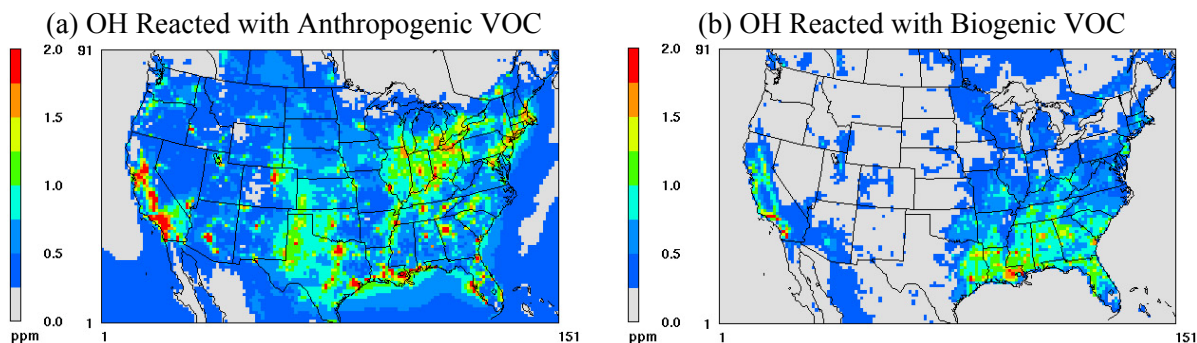


Figure 2. Spatial distributions of 15-day mean of (a) OH reacted with anthropogenic VOCs, and (b) OH reacted with biogenic VOCs predicted by CMAQ during June 14-28, 1999.

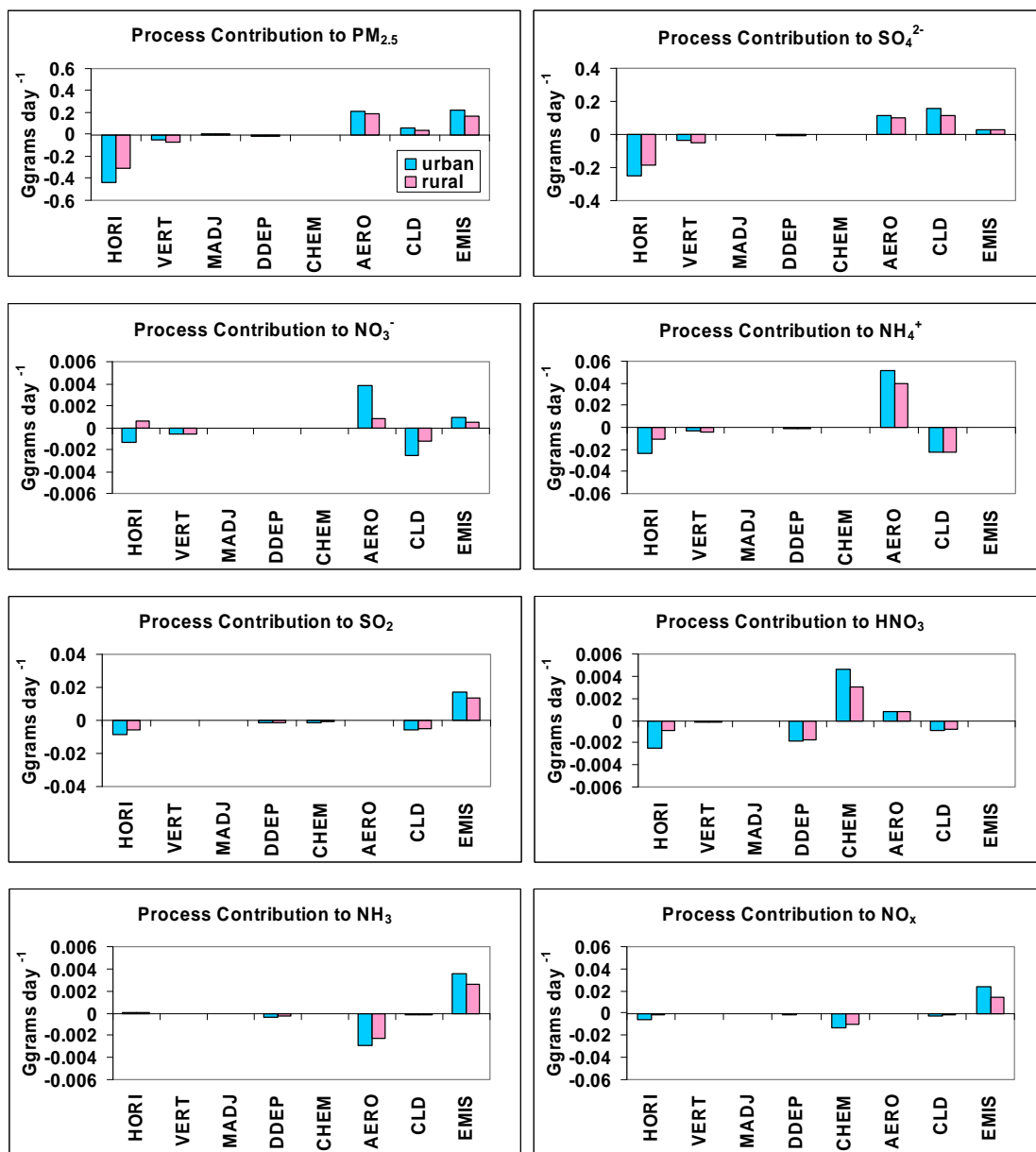


Figure 3. Contributions (Ggrams day<sup>-1</sup>) of horizontal transport (HORI), vertical transport (VERT), mass balance adjustment (MADJ), dry deposition (DDEP), gas-phase chemistry (CHEM), aerosol processes (AERO), cloud processes (CLD), and emissions (EMIS) to the concentration change of PM<sub>2.5</sub>, SO<sub>4</sub><sup>2-</sup>, NO<sub>3</sub><sup>-</sup>, NH<sub>4</sub><sup>+</sup>, SO<sub>2</sub>, HNO<sub>3</sub>, NH<sub>3</sub>, and NO<sub>x</sub> predicted by CMAQ at the SEARCH sites during June 14-28, 1999.

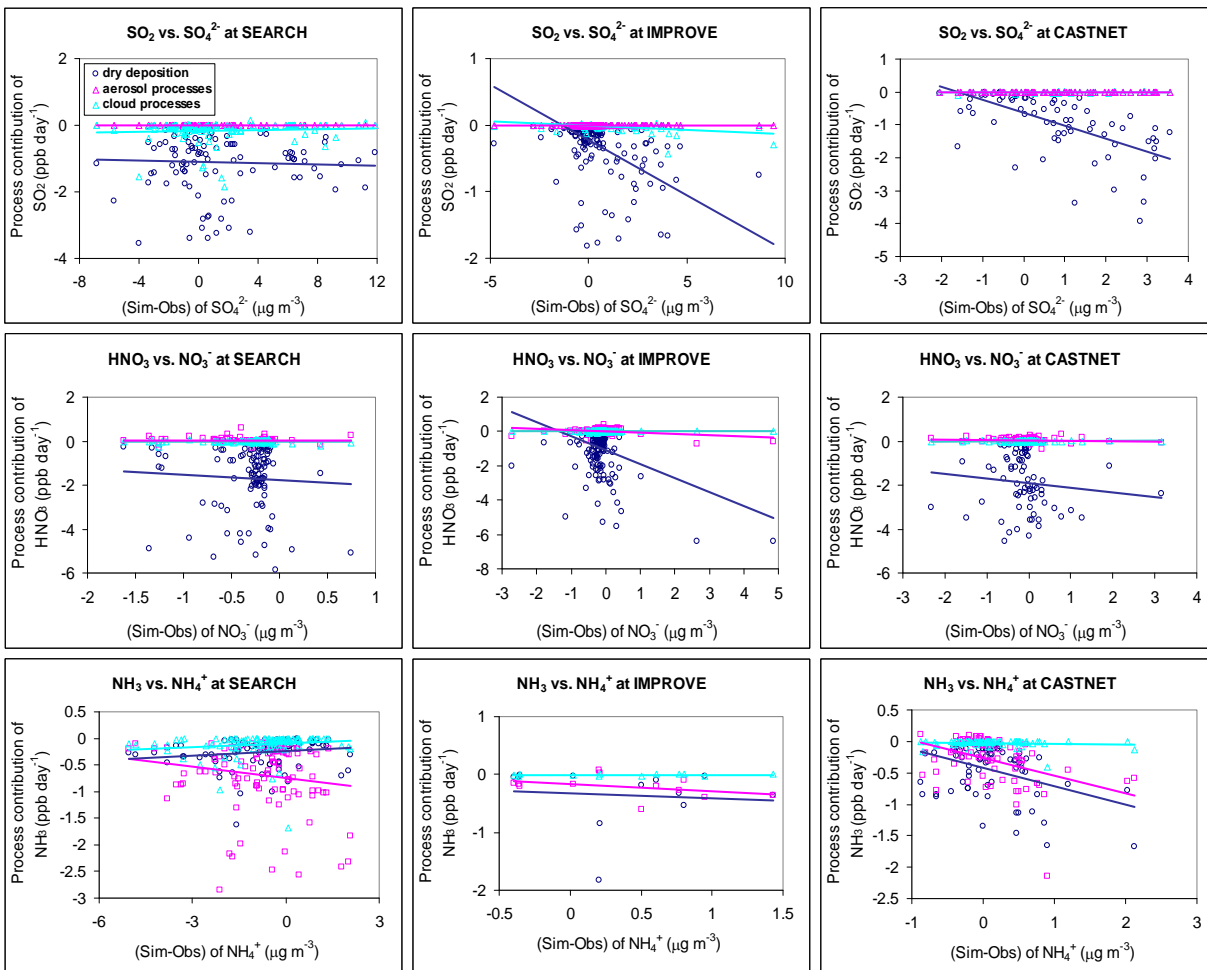


Figure 4. Scatter plots of process contributions of aerosol processes, cloud processes, and dry deposition of PM precursors (i.e.,  $\text{SO}_2$ ,  $\text{HNO}_3$ , and  $\text{NH}_3$ ) versus large model biases for corresponding PM (i.e.,  $\text{SO}_4^{2-}$ ,  $\text{NO}_3^-$ , and  $\text{NH}_4^+$ ) (by CMAQ), respectively, at the SEARCH, IMPROVE, and CASTNET sites during June 14-28, 1999.

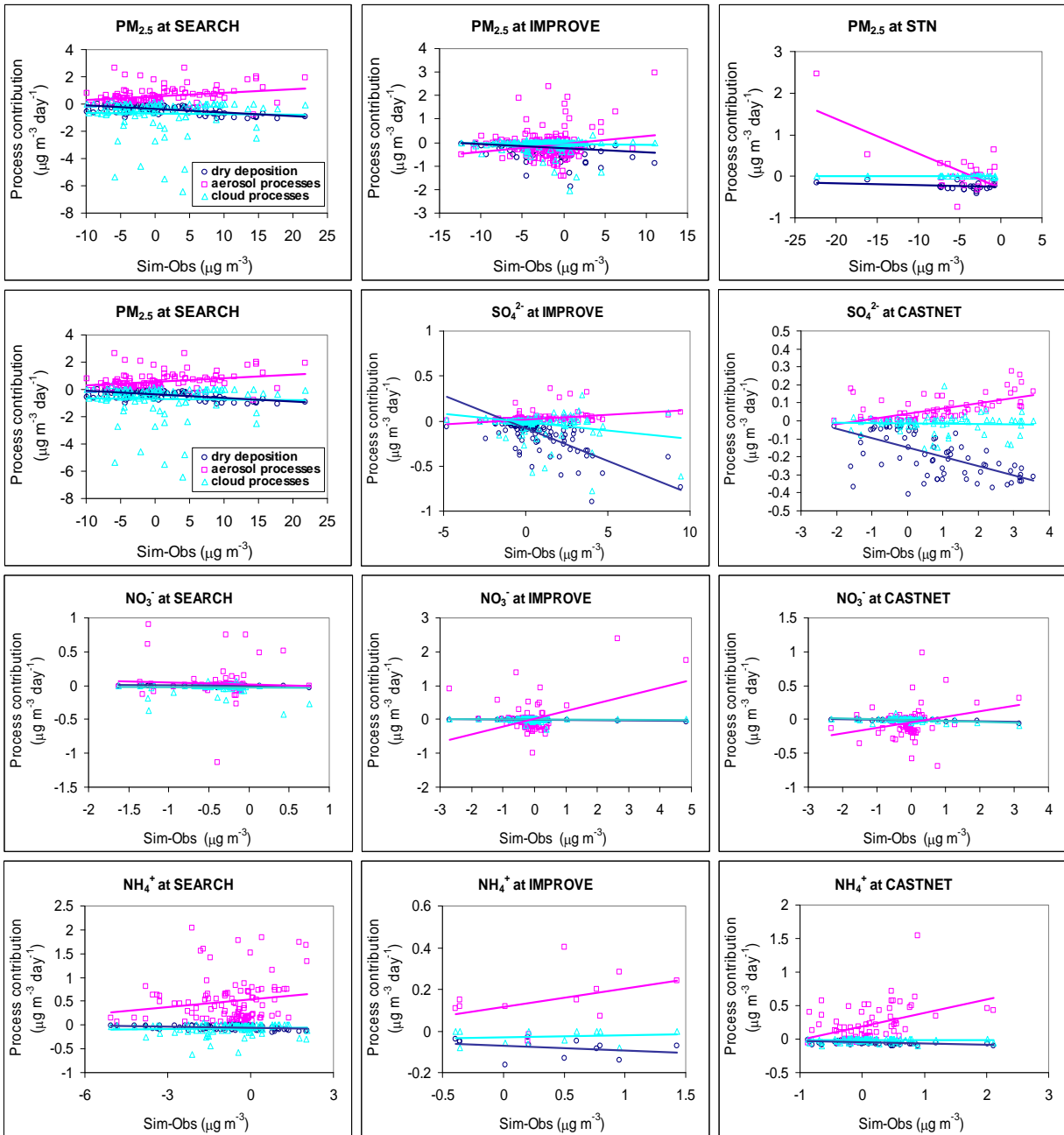


Figure 5. Scatter plots of process contributions of aerosol processes, cloud processes, and dry deposition versus large model biases for  $PM_{2.5}$ ,  $SO_4^{2-}$ ,  $NO_3^-$ , and  $NH_4^+$  (by CMAQ) at the SEARCH, IMPROVE, CASTNET, and STN sites during June 14-28, 1999. Observed  $PM_{2.5}$  is not available at the CASTNET sites, and observed PM components are not available at the STN sites for this episode.

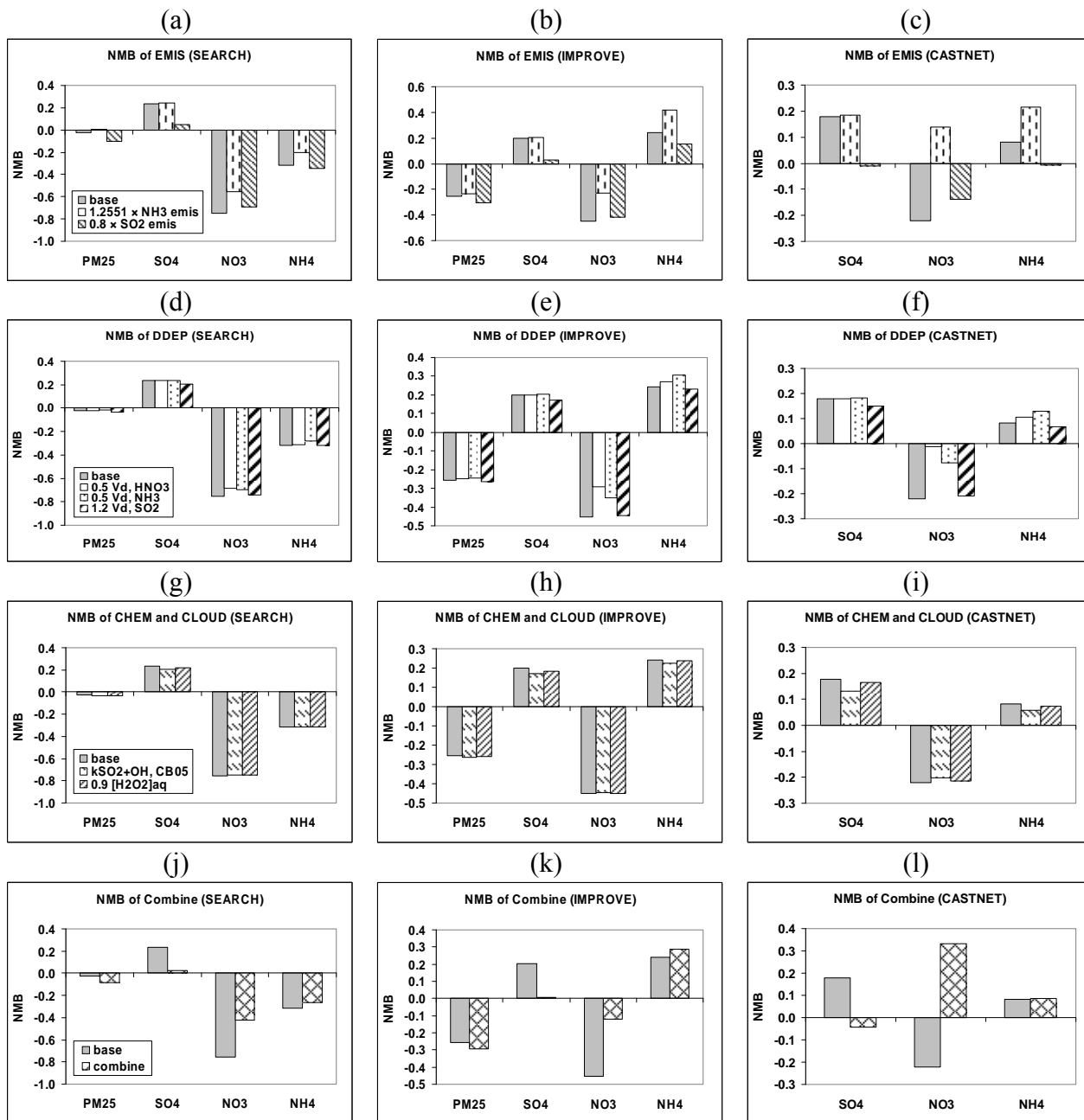


Figure 6. Normalized mean biases (NMBs) of simulated  $\text{NH}_4^+$ ,  $\text{NO}_3^-$ ,  $\text{SO}_4^{2-}$ , and  $\text{PM}_{2.5}$  (by CMAQ) for the baseline and various sensitivity simulations ((a)-(c): adjusting  $\text{NH}_3$  and  $\text{SO}_2$  emissions; (d)-(f): adjusting dry deposition velocity of  $\text{HNO}_3$ ,  $\text{NH}_3$ , and  $\text{SO}_2$ ; (g)-(i): replacing the rate constant of reaction  $\text{SO}_2$  and  $\text{OH}$ , and adjusting the dissolved concentrations of  $\text{H}_2\text{O}_2$  in cloud droplets; (j)-(l): multiple adjustments including  $1.2551 \times E_{\text{NH}_3}$ ,  $0.8 \times E_{\text{SO}_2}$ ,  $K_{\text{SO}_2+\text{OH}}$ ,  $\text{CB05}$ , and  $0.84 \times V_d$ ,  $\text{HNO}_3$ ) at the IMPROVE, SEARCH, and CASTNET sites in June 14-28, 1999. Observed  $\text{PM}_{2.5}$  concentrations are not available at the CASTNET sites.

**Supplementary data to be published online for the paper entitled:**

**Use of a Process Analysis Tool for Diagnostic Study on Fine Particulate Matter Predictions in the U.S. Part II: Process Analysis and Sensitivity Simulations**

Ping Liu<sup>a, b</sup> and Yang Zhang<sup>a, \*</sup>

<sup>a</sup> Department of Marine, Earth, and Atmospheric Sciences, North Carolina State University, Raleigh, NC 27695

<sup>b</sup> School of Environmental Science and Engineering, Shanghai Jiao Tong University, Shanghai, China

Shaocai Yu and Kenneth L. Schere

Atmospheric Sciences Modeling Division, the U.S. Environmental Protection Agency, Research Triangle Park, NC

---

\* Corresponding author: Yang Zhang, Department of Marine, Earth, and Atmospheric Sciences, Campus Box 8208, North Carolina State University, Raleigh, NC 27695; phone number: (919) 515-9688; fax number: (919) 515-7802; e-mail: yang\_zhang@ncsu.edu

## Appendix I

Table A-1. CMAQ Integrated Reaction Rate (IRR) outputs for the SAPRC-99 mechanism (modified from Byun and Ching, 1999).

<b>O<sub>x</sub> Budget</b>	
1. Total O <sub>x</sub> Pord	O <sub>x</sub> Chemical Production
2. Total O <sub>x</sub> Loss	O <sub>x</sub> Chemical Destruction
<b>Radical Initiation</b>	
3. newOH_O <sup>1</sup> D	new OH from O <sup>1</sup> D + H <sub>2</sub> O
4. newOHother	new OH from H <sub>2</sub> O <sub>2</sub> , HNO <sub>3</sub> , HONO, O <sub>3</sub> + HC (hydrocarbon except isoprene)
5. newHO <sub>2</sub> _HCHO	new HO <sub>2</sub> from HCHO
6. newHO <sub>2</sub> Tot	new HO <sub>2</sub> production (total)
7. newRO <sub>2</sub> Tot	new RO <sub>2</sub> production (total)
8. nHO <sub>x</sub> _isop	new HO <sub>x</sub> (including OH, HO <sub>2</sub> and RO <sub>2</sub> ) from isoprene
<b>Radical Propagation</b>	
9. OHwCO_CH <sub>4</sub>	sum of OH+CO and OH+CH <sub>4</sub> reactions
10. ISOPwOH	OH + ISOPRENE
11. ISOPwO <sub>x</sub>	isoprene reactions with O <sub>3</sub> , NO <sub>3</sub> and O <sup>3</sup> P
12. OH_VOC	OH reacted with anthropogenic VOC
13. OHw_all_HC	OH reacted with all VOCs including isoprene
14. OHpropmisc	other OH propagation reactions (e.g., OH + SO <sub>2</sub> )
15. HO <sub>2</sub> TotPord	total HO <sub>2</sub> Production
16. RO <sub>2</sub> TotPord	total RO <sub>2</sub> Production
17. HO <sub>2</sub> to NO <sub>2</sub>	NO <sub>2</sub> produced from reactions of HO <sub>2</sub>
18. HO <sub>2</sub> to OH	OH produced from reactions of HO <sub>2</sub>
19. RO <sub>2</sub> to NO <sub>2</sub>	NO <sub>2</sub> produced from reactions of RO <sub>2</sub>
20. OH_reacted	total OH production
<b>Radical Termination</b>	
21. OHterm	OH termination
22. HO <sub>2</sub> term	HO <sub>2</sub> termination
23. RO <sub>2</sub> term	RO <sub>2</sub> termination
24. H <sub>2</sub> O <sub>2</sub> Prod	production of H <sub>2</sub> O <sub>2</sub>
<b>Formaldehyde Production</b>	
25. HCHO <sub>p</sub> _isop	HCHO produced from isoprene reactions
26. HCHO <sub>p</sub> _Tot	HCHO produced from all reactions
<b>NO<sub>x</sub> Termination / Production</b>	
27. HNO <sub>3</sub> _OHNO <sub>2</sub>	OH + NO <sub>2</sub> → HNO <sub>3</sub>
28. HNO <sub>3</sub> _NO <sub>3</sub> HC	NO <sub>3</sub> + HC → HNO <sub>3</sub>
29. HNO <sub>3</sub> _N <sub>2</sub> O <sub>5</sub>	N <sub>2</sub> O <sub>5</sub> + H <sub>2</sub> O → 2HNO <sub>3</sub>
30. HNO <sub>3</sub> reacted	HNO <sub>3</sub> reacted (to produce NO <sub>x</sub> )
31. PANprodNet	net PAN prod
32. PANlossNet	net PAN loss (source of NO <sub>x</sub> and a radical)
33. RNO <sub>3</sub> _prod	production of organic nitrates
<b>Overall Oxidation Efficiency</b>	
34. OH_CL	OH chain length

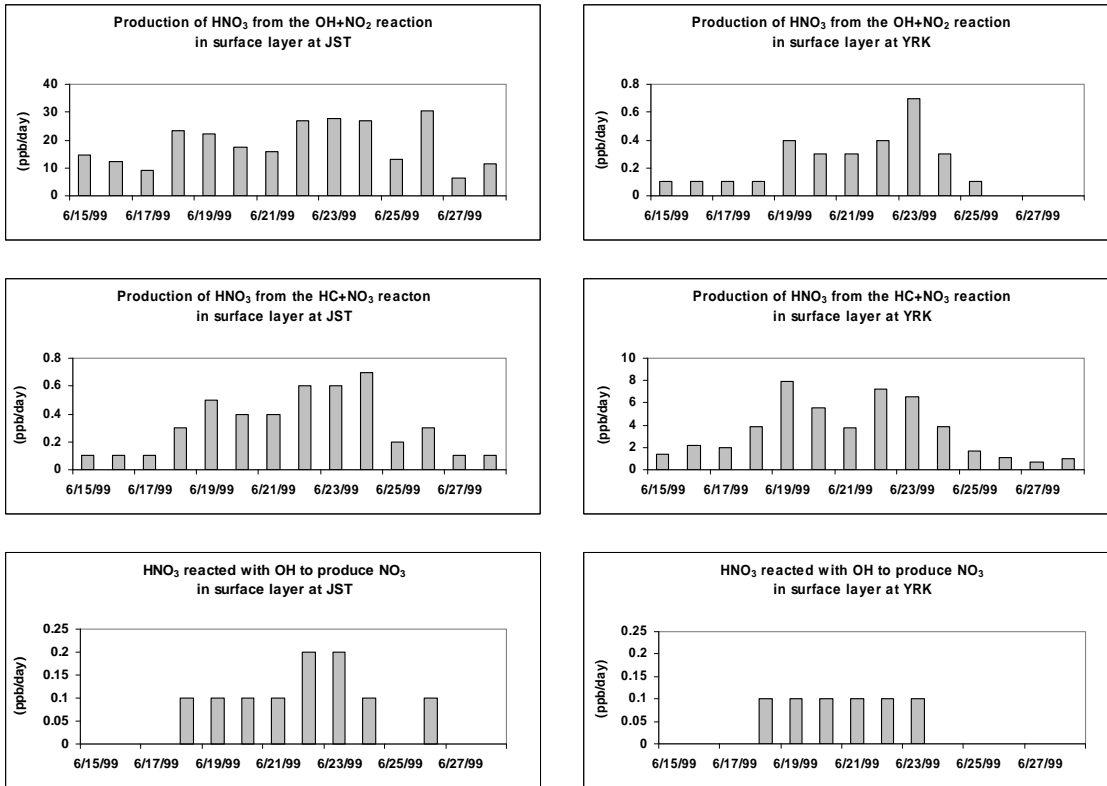


Figure A-1. Daily total production of HNO<sub>3</sub> from NO<sub>2</sub> reaction with OH and NO<sub>3</sub> reaction with HC, and HNO<sub>3</sub> reacted to produce NO<sub>3</sub> in the surface layer at JST, Atlanta, and YRK, GA, predicted by CMAQ during June 14-28, 1999.

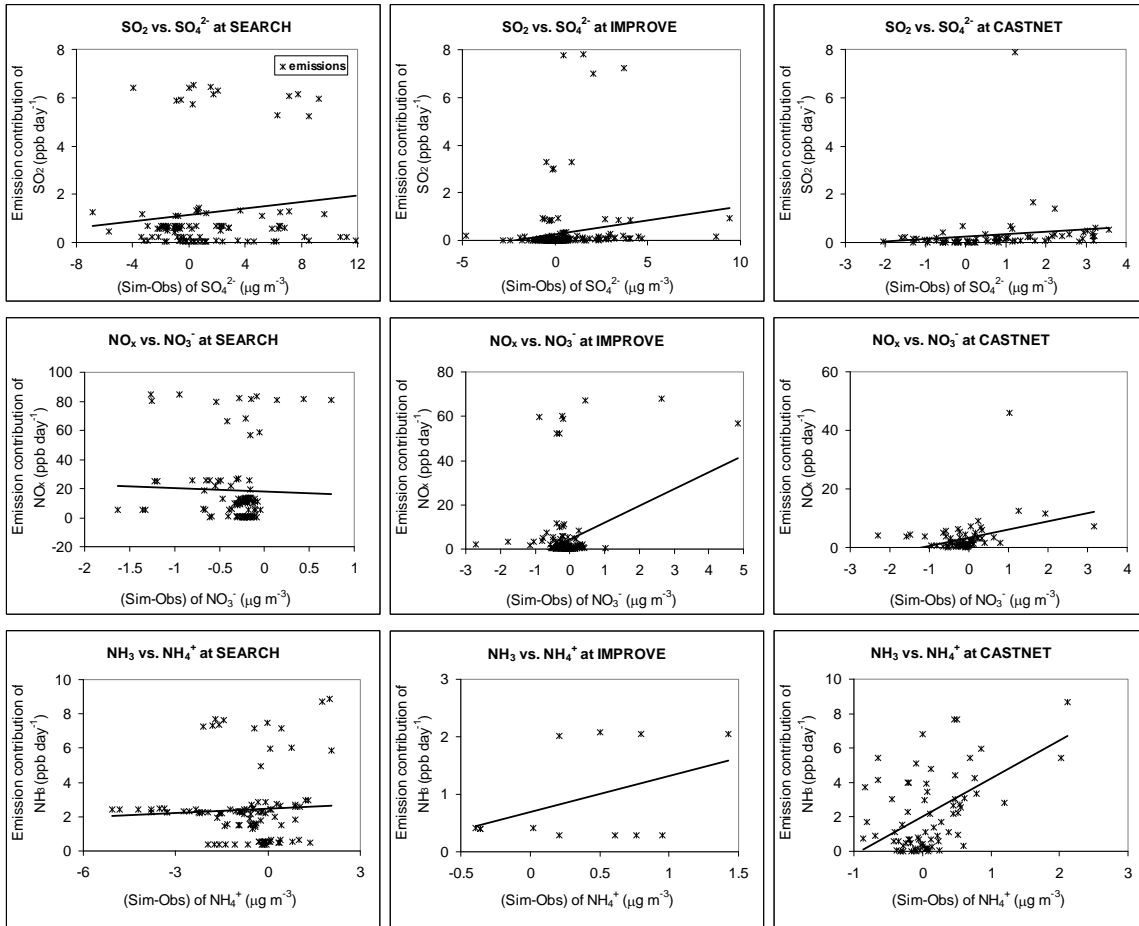


Figure A-2. Scatter plots of process contributions of emissions of PM precursors (i.e., SO<sub>2</sub>, NO<sub>x</sub>, and NH<sub>3</sub>) versus large model biases for corresponding PM species (i.e., SO<sub>4</sub><sup>2-</sup>, NO<sub>3</sub><sup>-</sup>, and NH<sub>4</sub><sup>+</sup>) (by CMAQ), respectively, at the SEARCH, IMPROVE, and CASTNET sites during June 14-28, 1999.

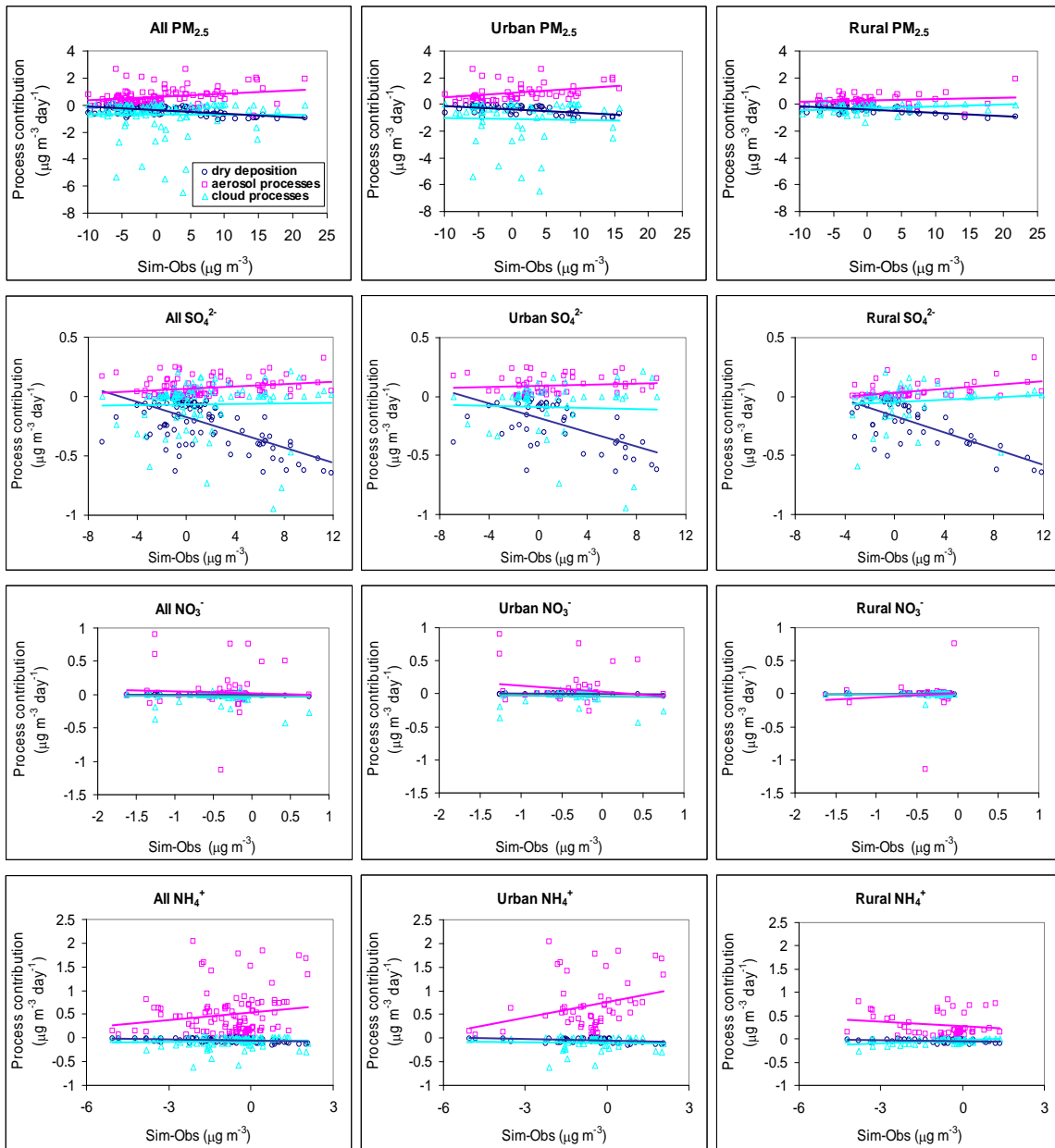


Figure A-3. Scatter plots of process contributions of aerosol processes, cloud processes, and dry deposition versus large model biases for  $PM_{2.5}$ ,  $SO_4^{2-}$ ,  $NO_3^-$ , and  $NH_4^+$  (by CMAQ) at SEARCH sites accounting for all, urban or rural sites separately during June 14-28, 1999.

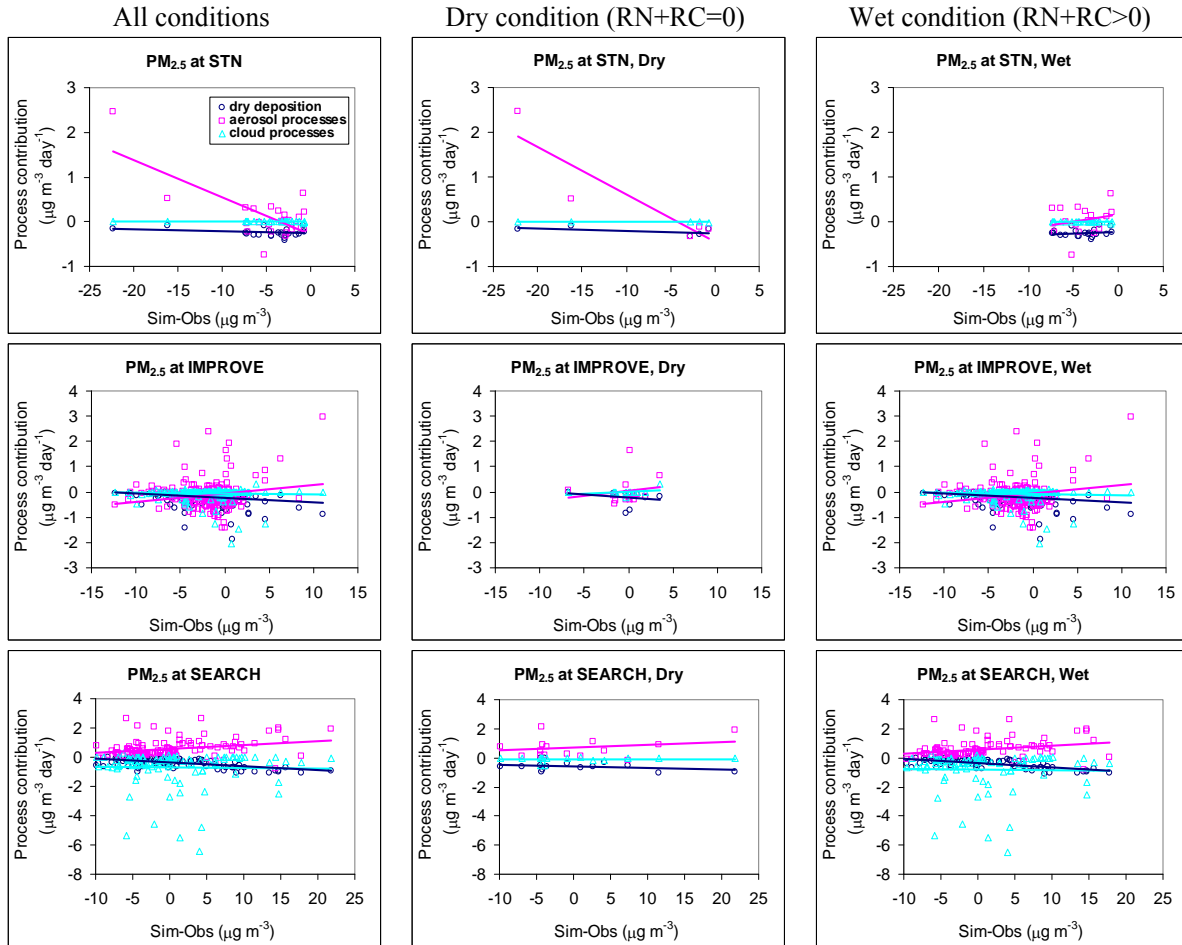


Figure A-4. Scatter plots of process contributions of aerosol processes, cloud processes, and dry deposition versus large model biases for PM<sub>2.5</sub> (by CMAQ) at all sites from STN, IMPROVE, and SEARCH under dry and wet conditions during June 14-28, 1999. RN and RC denote non-convective and convective precipitation. Dry and wet conditions correspond to  $RN + RC = 0$  or  $> 0$ , respectively.

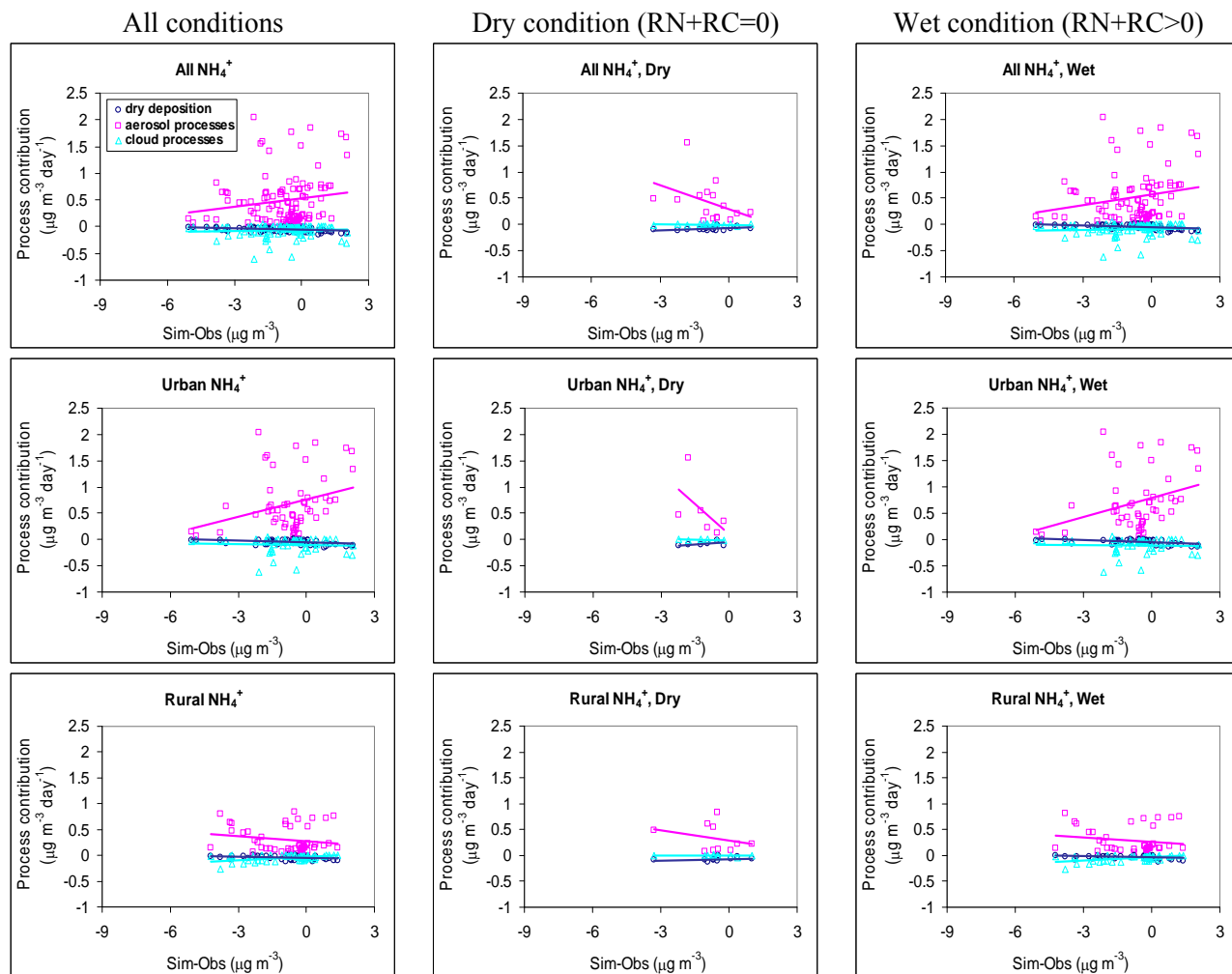


Figure A-5. Scatter plots of process contributions of aerosol processes, cloud processes, and dry deposition versus large model biases for  $\text{NH}_4^+$  (by CMAQ) at the SEARCH sites accounting for all, urban or rural sites separately under dry and wet conditions during June 14-28, 1999. RN and RC denote non-convective and convective precipitation. Dry and wet conditions correspond to  $\text{RN} + \text{RC} = 0$  or  $> 0$ , respectively.

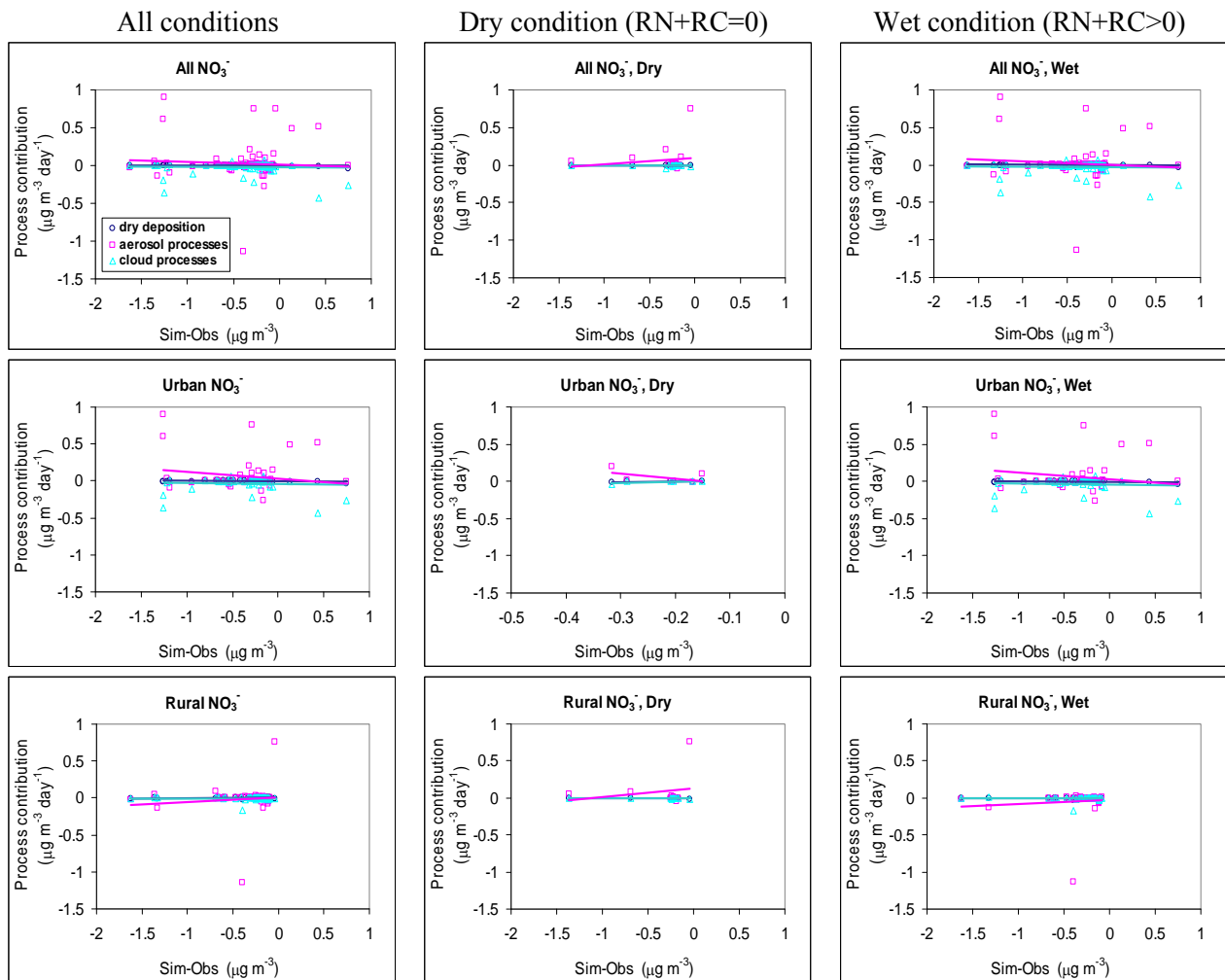


Figure A-6. Scatter plots of process contributions of aerosol processes, cloud processes, and dry deposition versus large model biases for  $\text{NO}_3^-$  (by CMAQ) at the SEARCH sites accounting for all, urban or rural sites separately under dry and wet conditions during June 14-28, 1999. RN and RC denote non-convective and convective precipitation. Dry and wet conditions correspond to  $\text{RN} + \text{RC} = 0$  or  $> 0$ , respectively.

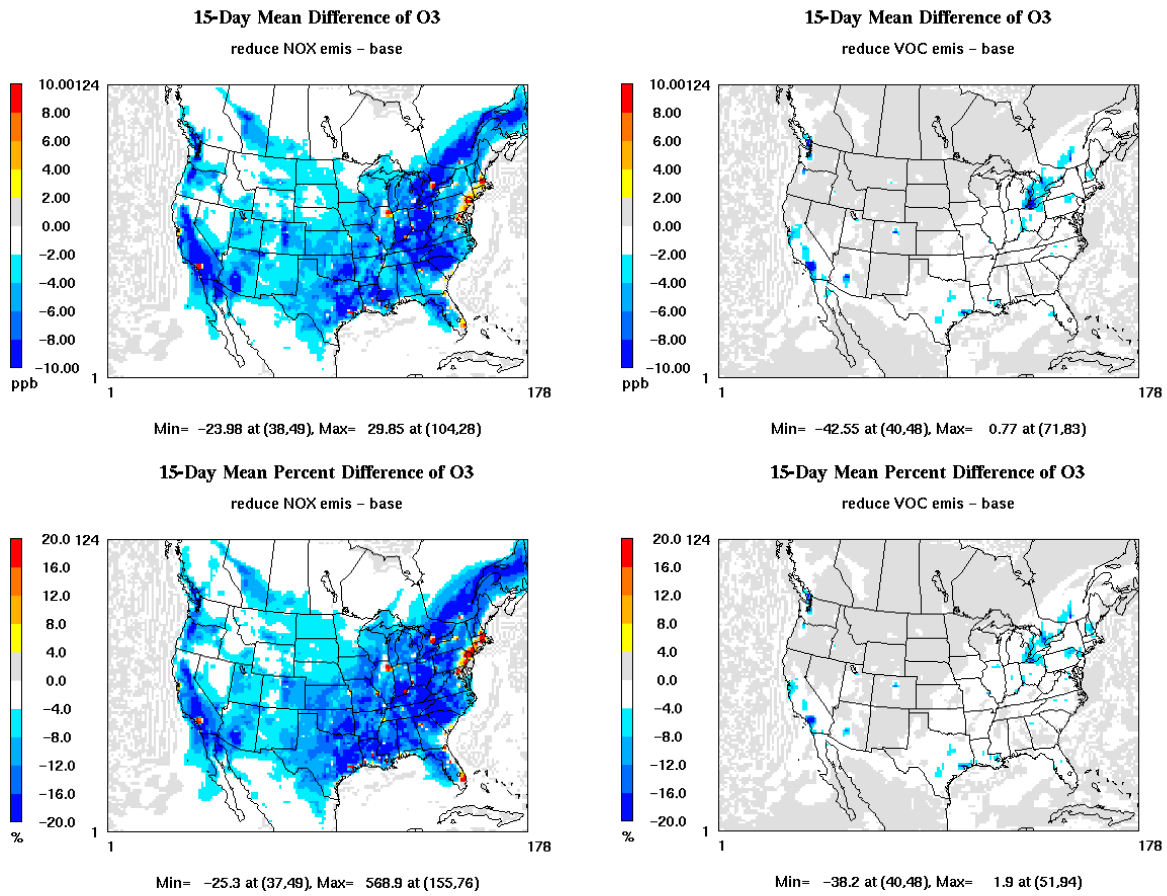


Figure A-7. Spatial distributions of 15-day mean of hourly O<sub>3</sub> from CMAQ baseline and simulations with 50% reduction of NO<sub>x</sub> and VOC emissions, and the absolute and percentage difference of hourly O<sub>3</sub> between the CMAQ simulations with 50% reduction of NO<sub>x</sub> and VOC emissions and the baseline simulation in June 14-28, 1999.